RESEARCH MEMORANDUM

INTERFERENCE EFFECTS OF FUSELAGE-STORED MISSILES ON INLET DUCT MODEL OF AN INTERCEPTOR-TYPE AIRCRAFT AT MACH NUMBERS 1.5 TO 1.9

By Thomas G. Piercy and Owen H. Davis

Lewis Flight Propulsion Laboratory
Cleveland, Ohio

NATIONAL ADVISORY COMMITTEE
FOR AERONAUTICS

WASHINGTON
April 24, 1957

NATIONAL ADVISORY COMMITTEE FOR AERONAUTICS

RESEARCH MEMORANDUM

INTERFERENCE EFFECTS OF FUSELAGE-STORED MISSILES ON INLET DUCT MODEL OF AN INTERCEPTOR-TYPE AIRCRAFT AT MACH NUMBERS 1.5 TO 1.9

By Thomas G. Piercy and Owen H. Davis

SUMMARY

The effect of missile armament on the performance of an interceptor-type aircraft model has been determined at Mach numbers 1.5, 1.7, and 1.9 and at angles of attack to 19°. With this configuration missiles were carried in a bay located on the bottom of the aircraft fuselage and mounted to a rotatable missile door. Rotation of the door then brought the missiles into the external or firing position.

The aircraft model was characterized by triangular-shaped normal-shock inlets located at the wing roots. Relatively short and curved subsonic diffusers fed simulated twin side-by-side turbojet engines. Inasmuch as the missile bay extended considerably ahead of the inlet station, rotation of the missile door created considerable disturbance of the flow entering the inlets.

In comparison with the internal missile arrangement, the external missile configurations increased the model lift, drag, and pitching moment. While the diffuser-exit flow distortion and static-pressure fluctuations were not greatly affected, diffuser total-pressure recovery was reduced as much as 0.058 at Mach number 1.9 for one missile configuration.

The most detrimental effect of missile-door rotation occurred at the transient door positions, or with the door halfway between the missiles-in and -out conditions. At this door position the flow into the inlets was highly asymmetrical. Although the performance of both left and right ducts was generally reduced, the inlet duct on the cavity side of the missile door was most severely penalized, becoming unstable at relatively low angles of attack and with resulting large pressure-recovery losses and increases in flow distortion. The installation of fuselage fences along the missile bay was only partially effective in reducing these losses.

INTRODUCTION

The external transport of stores by aircraft causes drag penalties and possible aircraft trim changes when the stores are dropped (e.g., ref. 1). An obvious method of eliminating this drag penalty for a missile carrier is to house the missiles internally through the cruise-out phase of the flight plan and to expose the missiles externally for a relatively short time during combat.

In this investigation several missile configurations were housed in a missile bay located on the bottom of an interceptor-type aircraft fuselage. The missiles were located on the bay door, which was rotatable to bring the missiles into firing position. This door extended considerably ahead of the inlet station, so that, with partial door rotation or with the missiles in firing position, considerable obstruction to the flow entering the inlets was possible.

The primary purpose of these tests was to determine the effect of the missile-door rotation and various missile arrangements on the performance of the duct system. Limited drag, lift, and pitching-moment data were also obtained.

Tests were run in the 8- by 6-foot tunnel at the NACA Lewis laboratory. Data were obtained at Mach numbers 1.5, 1.7, and 1.9 and at angles of attack to 19°.

SYMBOLS

A	area
A_C	compressor-face area, 0.0789 sq ft
A_i	inlet throat area, 0.0735 sq ft
A_W	complete wing area, 5.76 sq ft
C_D	drag coefficient, D/q_0A_W
C_L	lift coefficient, L/q_0A_W
C_M	pitching-moment coefficient, $\overline{M}/q_0A_W\overline{c}$
$\overline{c}$	wing mean aerodynamic chord, 1.28 ft
D	drag, lb

L	lift, lb
M	Mach number
$\overline{M}$	pitching moment, ft-lb
m/m_0	mass-flow ratio, $\rho_i V_i A_i / \rho_0 V_0 A_i$
P	total pressure
ΔP	difference between maximum and minimum total pressure at rake station
$\Delta P/P_{av}$	distortion parameter
Δp	variation of static pressure at pressure transducer
$\Delta p/p_{av}$	duct static-pressure-fluctuation parameter
q	dynamic pressure, lb/sq ft
V	velocity, ft/sec
w	weight flow, lb/sec
y	height normal to fuselage surface
α_b	angle of attack of fuselage, deg
β	missile-door position, deg
δ	ratio of total pressure to NACA standard sea-level pressure
θ	ratio of total temperature to NACA standard sea-level temperature
ρ	density of air, slugs/cu ft

Subscripts:

av	average
f	with fuselage fences
i	inlet throat
l	local
0	free stream
2	compressor-inlet station

APPARATUS AND PROCEDURE

Model

A schematic drawing of the aircraft model tested is presented in figure 1. Air to two simulated turbojet engines was supplied through separate ducting by normal-shock wing-root inlets. The inlets were sized for transonic cruise conditions; and, since no bypass system was provided, subcritical inlet operation resulted at supersonic speeds. The inlets were provided with a conventional fuselage boundary-layer-removal system consisting of an open-nose wedge diverter beneath the splitter plate. Air taken on board through the diverter system was immediately returned to the free stream by means of an exit on the bottom of the fuselage.

As indicated, the model included a portion of the configuration wing. The incidence of the wing-chord plane was 1° with respect to the fuselage centerline. The missile bay was located on the bottom of the fuselage ahead of the inlet station. Missiles of the types shown in figure 2 were mounted to the missile bay door, which was rotatable to bring the missiles into the external firing position.

Photographs of the model with various missile arrangements and door positions are presented in figure 3. For convenience, a table of configurations is listed in figure 4, which schematically shows cross sections through the model at the missile bay section for typical armament and door rotations.

Figure 3(a), a photograph of the configuration schematically shown in figure 1, represents the condition of internal missile storage. The fairings on the missile door are covers fitting over the missile fins. This photograph then represents the $A_{1,f}$ configuration at β of 0°. Without the missile fin covers and fuselage fences the configuration would be identical to A_0. The same missile arrangement but with missiles rotated 180° to the firing position is indicated in figure 3(b).

In order to rotate the missile door so that the missiles are put in firing position, the door must pass through the intermediate position indicated in figure 3(c). The direction of missile door rotation is shown in figure 4(a).

The alternate missile arrangement using type II missiles is shown in figures 3(d) and 4(c). For this missile arrangement the model was tested only with the missiles in the firing position (β of 180°).

The variation of diffuser flow area for one duct is presented in figure 5. The slight internal contraction from the inlet lip to the inlet-throat station is neglected in this figure.

The balance (fig. 1), with balance center at fuselage station 48.39 and water line 9.38, measured two lift components and one drag component. Internal forces and base pressures were subtracted from the balance readings so that lift and drag coefficients represent external forces only. The center of moments was taken at station 49.27, or at 28.57 percent of the wing mean aerodynamic chord. All force coefficients were based on the complete wing area of 5.76 square feet, although the tests were run with the stub wing. Force results therefore do not represent absolute airplane forebody values but are useful in determining force-component changes with various missile arrangements.

Instrumentation

Duct total-pressure recovery was determined with area-weighted Pitot-static rakes at fuselage station 50.09 in both left and right ducts. Inlet mass flow was remotely varied with exit plugs and was calculated from static-pressure measurements at station 61.39 assuming choked conditions at the exit plugs. Signals from pressure transducers were photographed on film for determination of duct instability. These transducers were located on the inboard duct walls (fig. 1).

Flow conditions ahead of the inlet and at the inlet-throat station were determined with the instrumentation shown in figure 6. The fuselage boundary layer and the flow ahead of the inlet face were determined with rakes and wedge bars, respectively, ahead of the left side inlet. Simultaneous flow surveys at the throat of the inlet were determined by rakes mounted in the right inlet. The boundary-layer rakes and wedge bars were mounted on rotatable pads. Rotation of the pads was necessary to maintain flow attachment on the wedge bars as the model angle-of-attack range was changed.

Procedure

With a given missile arrangement, the model was run through the range of angle of attack, door position, and Mach number. All data reported herein were taken for corrected engine weight flows corresponding to 35,000-feet altitude for a current two-spool turbojet engine operating at military power. Inlet mass flow is not used as a plotting variable in this report. However, the inlet mass flow for any data point may be obtained from figure 7, which presents the relation between duct over-all pressure recovery and inlet mass-flow ratio at the engine match conditions. This mass-flow ratio represents the ratio of the inlet mass flow to the mass flow through an area equivalent to the inlet-throat area at free-stream conditions, or

$$\frac{m}{m_0} = \frac{\rho_i V_i A_i}{\rho_0 V_0 A_i}$$

Owing to excess model blockage at angle of attack, tests could not be conducted at Mach 1.5 at angles of attack greater than about 10°. Force data were obtained only for angles of attack up to 8° because of balance failure. Owing to the asymmetric flow conditions at partial door rotations, the missile door was rotated through 360° to complete the survey of the flow conditions at the inlet.

RESULTS

Force Measurements

Effects of missile armament and missile-door rotation on model force and moment coefficients are summarized in figure 8. In comparison with the unarmed vehicle A_0, all armament additions caused noticeable increases in model lift and drag forces. The drag coefficient was increased as much as 0.009 and the lift coefficient as much as 0.030 by door rotation from the missile-in condition in the angle-of-attack range investigated. (Force components for the A_2 configurations were not appreciably different from those for the A_1 configuration at β of 180° and therefore are not presented.) It will be noted that even the addition of the missile covers to the door (configuration A_1 at $\beta = 0^{\circ}$ compared with A_0) caused some drag and lift increases.

Nose-up pitching-moment increases were small, and it appears that changes in static pitching stability dC_M/dC_L would be small for any of these armament configurations.

Effect of Armament on Inlet-Duct Performance

The duct performance of all configurations is summarized in figures 9. Performance parameters include the over-all duct pressure recovery, flow distortion at the compressor inlet, and the duct static-pressure fluctuation, each plotted as a function of angle of attack. Data for the A_1 configuration for which the missile door was rotated are cross-plotted against door position β in figure 10.

There was usually some flow dissimilarity between left and right ducts even when the configuration was symmetrical. This dissimilarity was particularly noticeable at Mach number 1.9 for $\beta = 0^{\circ}$ (fig. 9(e)). An examination of the model revealed no significant differences between the left and right ducts, and hence the reasons for this dissimilarity are not known.

It will also be noted in figures 9 and 10 that occasionally the static-pressure fluctuations are shown by dashed curves. These represent

extrapolations at low values of the parameter for which no data were taken.

An examination of the data of figure 9 indicates that, generally, for symmetrical external flow conditions ($\beta = 0^\circ$ or 180°), the duct performance parameters varied only slightly for angles of attack up to about 11° or 12°. For larger angles of attack, however, the inlet recovery dropped rapidly while the distortion and static-pressure fluctuation increased. When the missile door was at 90°, the angle of attack at which the duct performance suddenly deteriorated (hereafter termed the critical angle of attack) was reduced. For example, at Mach 1.7 for the A_1 configuration, the critical angle of attack was decreased about 2° for the right duct and about 6° for the left duct (fig. 9(c)). At Mach number 1.9 a similar comparison gives about a 7° decrease for the right duct and about 11° for the left duct (fig. 9(f)). In addition, at Mach 1.9 the left duct operated at considerably lower recovery than the right duct. Examination of figure 4 shows that for $\beta = 90^\circ$ the missiles were next to the right-side inlet, and the cavity caused by door rotation was on the left side. Hence, the inlet on the cavity side of the missile door was more severely penalized by missile-door rotation.

For angles of attack less than the critical values the differences in duct performance between the various missile configurations for β of 0° were generally small, since externally the configuration was changed only by the addition of missile fairing covers or fuselage fences. The peculiar right-duct performance at Mach 1.9 is an exception to this general observation. With the missiles rotated into firing position ($\beta = 180^\circ$) a considerable difference in the duct total-pressure recovery was noted between configurations, although again there were no major changes in distortion level or static-pressure fluctuations. The least loss of pressure recovery (about 0.01) in comparison with the unarmed configuration occurred with configuration A_2 (see figs. 9(d) and (g)). For configurations A_1 or $A_{1,f}$ these pressure-recovery losses were as high as 0.034, 0.046, and 0.058 at Mach numbers 1.5, 1.7, and 1.9, respectively (figs. 9(a), (d), and (g)).

For angles of attack greater than the critical values, large differences in duct pressure recovery, distortion, and buzz occurred among armament configurations. The results showed very little consistency. At Mach 1.7 for $\beta = 0^\circ$ (fig. 9(b)) the addition of fuselage fences increased the critical angle of attack from 11° or 12° to about 15° or 16°. For β of 180° the use of fuselage fences was either ineffective or detrimental (fig. 9(d)). At the transient door position of 90° the fuselage fences improved somewhat the pressure recovery and flow distortion of the left inlet at the higher angles of attack but proved inconsistent in reducing the static-pressure fluctuations (figs. 9(c) and (f)).

The effects of door rotation on duct performance may be more easily observed in figure 10, where the previous data are replotted against door position β for configuration A_1. (Data for intermediate door positions at Mach 1.5 previously omitted are included in these plots.) In general, the effect of door position on duct performance increased as the Mach number and angle of attack increased. The intermediate door position of 90°, in general, produced the largest flow distortions and static-pressure fluctuations.

At angles of attack below 11° the flow distortions and static-pressure fluctuations for missiles-out were not greatly different from the missiles-in results. The duct pressure recoveries, however, were consistently lower for the missiles-out data.

Fuselage Boundary-Layer Survey

In an attempt to understand some of the foregoing results, the flow immediately ahead of the left inlet was surveyed with the instrumentation of figure 6. For door positions of 0° or 180° the flow was assumed to be asymmetrical, and hence the results apply to the flow entering either inlet. For the door position of 90°, however, the flow survey represents data for the cavity-side inlet. A corresponding door position of β of 270° was therefore tested in order to determine the flow conditions ahead of the missile-side inlet. Typical total-pressure profiles and flow deflection angles immediately ahead of the inlet are presented in figures 11 and 12 for the A_1 configuration for several door positions. Occasionally the data are extrapolated at the larger angles of attack. These extrapolations represent conditions for which attached supersonic wedge flow data were not obtained.

An examination of the total-pressure profiles of figure 11 indicates large differences in the vicinity of the fuselage surface due to missile-door rotation. When the missile door was rotated 90° the boundary layer thickened noticeably on the cavity side of the door, with the result that larger amounts of boundary layer entered the inlets. (The approximate boundary-layer splitter-plate height is indicated on the ordinate of fig. 11.) The effects of door rotation on the missile-side inlet profiles, however, were rather small by comparison for the range of angle of attack studied. This thickening of the fuselage boundary layer on the cavity-side inlet therefore partially explains its reduced performance. Somewhat thicker boundary layers were also measured for β of 180° in comparison with the 0° door position, particularly at high angles of attack. The profiles for configuration A_0 were essentially the same as for A_1 at β of 0° and hence are not presented.

Typical local flow deflections at the inlet station are presented in figure 12 for Mach numbers 1.7 and 1.9. The data show that, in general, the local flow deflection increased more rapidly than the angle of attack. (This is a typical result of crossflow.) In addition, the highest flow deflections were measured consistently with the lower wedge bar. As with the total-pressure profiles, large differences in flow deflections were noted between the various configurations, the largest deflections being observed with the β of 90° configuration.

Local Mach numbers ahead of the inlet were consistently lower than the free-stream values. Average Mach number decrements were about 0.05 and 0.10 at Mach numbers 1.7 and 1.9, respectively. The least Mach number reduction occurred with the 180° door position, while the largest reduction occurred on the cavity side for 90° door rotation. Inasmuch as these data do not assist in analyzing the results, they have not been plotted for this report.

Total-Pressure Contours at Inlet Throat and Diffuser Exit

Typical total-pressure contours at the inlet throat and compressor-inlet station are presented in figure 13 for the A_1 configuration at Mach number 1.7. Although data for the two rake stations were not taken simultaneously, each set of data represents very nearly the same inlet operating condition.

Data are presented for door positions of 0°, 90°, and 180° for angles of attack from 2° to 19°. At low angles of attack the lowest total pressure at the inlet throat was measured on the inboard inlet side about halfway between the upper and lower inlet corners. This result is believed to be due to the thicker fuselage boundary layer in this location (see fig. 11). As the angle of attack was increased, the general level of recovery at the throat began to decrease, with a very rapid decrease occurring in the lower inboard corner. For β of 0° the lower inboard corner had completely filled with separated air for angles of attack greater than 11°. Similar results were observed for the other door positions, although the angles of attack at which the flow separations occurred were considerably lower for door position 90°. The occurrence of this separation at the inlet throat may logically be assumed to be the cause of the pressure-recovery losses and large increases in distortion previously noted at the compressor inlet.

The breakdown of inlet performance at the higher angles of attack may thus be related to a flow breakaway in the lower inboard corner of the inlet. This conclusion is in agreement with the flow survey data of figure 12, which showed large flow deflections with the lower survey rake. The addition of missiles to the lower side of the fuselage appears to aggravate this condition by increasing the amount of boundary

layer entering the inlets (fig. 11) and by increasing the local flow deflections. It is not clear, however, why the fuselage-fence configuration ($A_{1,f}$) was not consistent in improving this condition.

Concluding Remarks

The breakdown of performance for the unarmed configurations at high angles of attack appears to result from adverse effects of body cross-flow, which caused separation at the inlet throat. Redesign of the lower inboard lip or the use of boundary-layer suction in this region could feasibly improve the performance at high angles of attack.

The most severe performance penalties occurred for the intermediate missile-door position ($\beta = 90^{\circ}$). Inasmuch as the missile door may be rotated on an actual airplane from the missiles-in to the missiles-out condition in a matter of seconds, the true import of these performance penalties cannot be evaluated herein. The most serious result of missile-door rotation on a tactical airplane would be the possibility of engine surge or stall due to the poor flow profiles entering the compressor, causing afterburner blowout. Such an evaluation could be carried out only by flight testing.

The data selected to be presented were obtained for corrected engine weight flows corresponding to an altitude of 35,000 feet, resulting in subcritical inlet operation. Actually, test data were taken for a range of weight flows bracketing the desired values. It was consistently observed that the critical angle of attack was increased as the corrected weight flow was increased (inlet operating at higher mass-flow ratio). This result, then, indicates at least two possible methods of reducing the observed effects of missile armament on the duct performance: (1) the use of smaller inlets or (2) the use of a bypass ahead of the compressor station.

SUMMARY OF RESULTS

The effects of missile armament on the performance of an interceptor-type aircraft have been determined at Mach numbers 1.5, 1.7, and 1.9 and at angles of attack to 19°. The aircraft was characterized by normal-shock wing root inlets feeding twin turbojet engines through rather short and highly curved subsonic diffusers. For this configuration, missiles were carried internally in a missile bay located on the bottom of the fuselage, which extended considerably ahead of the inlets. Rotation of the missile door through 180° then brought the missiles into firing position.

All data were taken for corrected engine weight flows corresponding to a 35,000-foot altitude for a current two-spool engine operating at military power. The effects of missile armament and door position may be summarized as follows:

1. With the clean or unarmed airplane, operation at angle of attack was generally limited to about 11° or 12°. Beyond this range the inlets became unstable and duct pressure recovery decreased rapidly while flow distortion increased rapidly. This sudden decrease in performance appeared to be associated with the onset of flow separation at the inlet throat.

2. When the missile door was rotated so that the missiles were external, duct distortion and flow fluctuation at angle of attack were changed only slightly from the clean configuration. Duct pressure recovery was reduced, however, as much as 0.058 for one missile configuration at Mach number 1.9. The least change in pressure recovery was about 0.01 with another configuration.

3. The largest performance losses occurred when the missile door was positioned halfway between the missiles-in and missiles-out conditions. With this door location, flow into the inlets was asymmetrical. Although the performance of both ducts was generally reduced, the inlet duct on the cavity side of the missile door was most severely penalized. Rotation of the missile door caused the cavity-side inlet to become unsteady at relatively low angles of attack, with resulting large pressure-recovery drops and increases in flow distortions. The installation of fuselage fences reduced these effects only slightly.

4. In general, rotation of the missile door increased the drag, lift, and pitching moment of the configuration. The drag coefficient was increased as much as 0.009 and the lift coefficient as much as 0.030 for the intermediate or missiles-out configuration in comparison with the clean airplane.

Lewis Flight Propulsion Laboratory
National Advisory Committee for Aeronautics
Cleveland, Ohio, January 18, 1957

REFERENCE

1. Rainey, Robert W.: Investigation of the Effects of Bomb-Bay Configuration Upon the Aerodynamic Characteristics of a Body with Circular Cross Section at Supersonic Speeds. NACA RM L55E27, 1955.

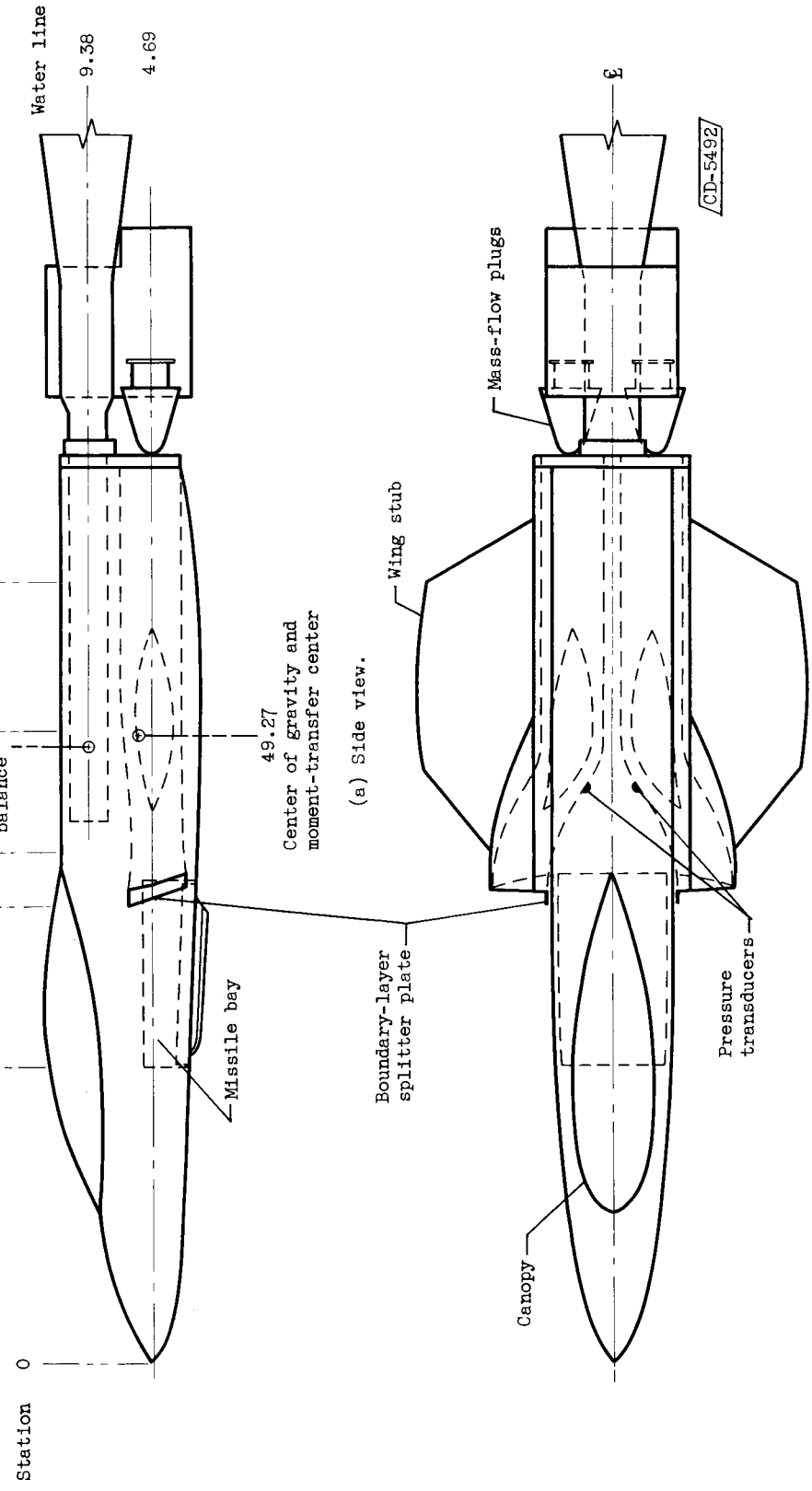

Figure 1. - Schematic drawing of model (dimensions in inches).

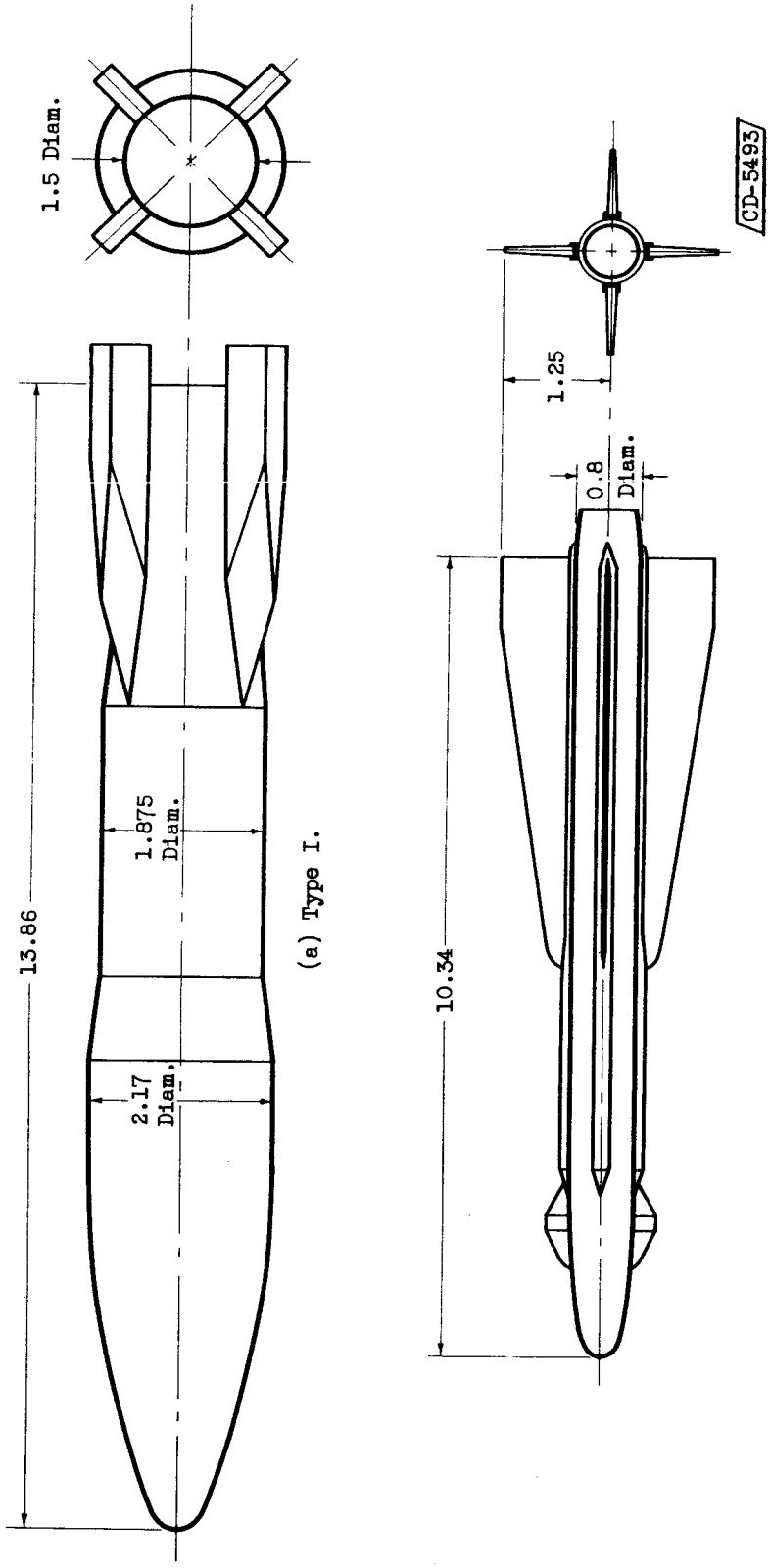

Figure 2. - Missile configurations (dimensions in inches).

(a) Configuration $A_{1,f}$ at β of 0°.

(b) Configuration $A_{1,f}$ at β of 180°.

(c) Configuration $A_{1,f}$ at β of 270°.

(d) Configuration A_2 at β of 180°.

Figure 3. - Photographs of model with typical missile arrangements and missile-door positions.

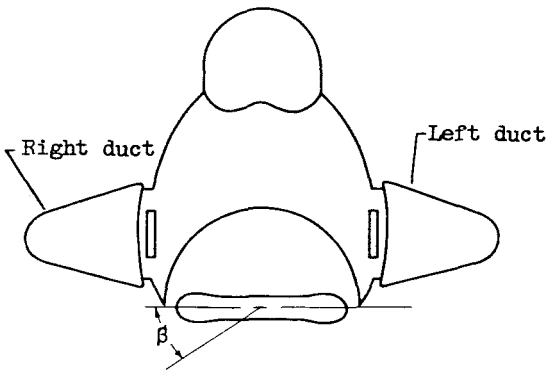

(a) Unarmed A_0; $\beta = 0^\circ$.

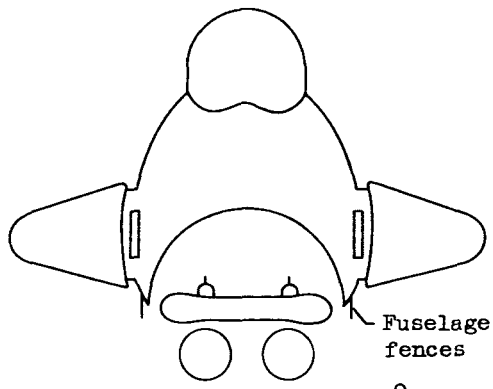

(b) Armed $A_{1,f}$; $\beta = 180^\circ$.

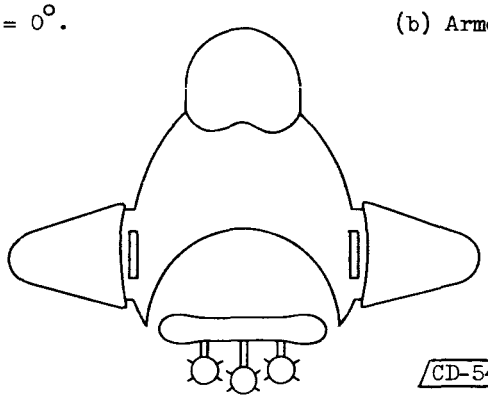

(c) Armed A_2; $\beta = 180^\circ$.

Configuration	Description	β	Photograph
A_0 (fig. 4(a))	Unarmed clean configuration	0° Only	Same as fig. 3(a) but without missile fin covers
A_1	2 Type I missiles (fig. 2(a)); 2 missile fin covers on outside of missile door	0°, 90°, 180°, 270°	Same as figs. 3(a), (b), and (c) with exception of fuselage fences
A_2 (fig. 4(c))	3 Type II missiles (fig. 2(b))	180° only	Fig. 3(d)
$A_{1,f}$ (fig. 4(b))	Same as A_1, fuselage fences added	0°, 90°, 180°, 270°	Figs. 3(a), (b), and (c)

Figure 4. - Missile arrangements and door positions.

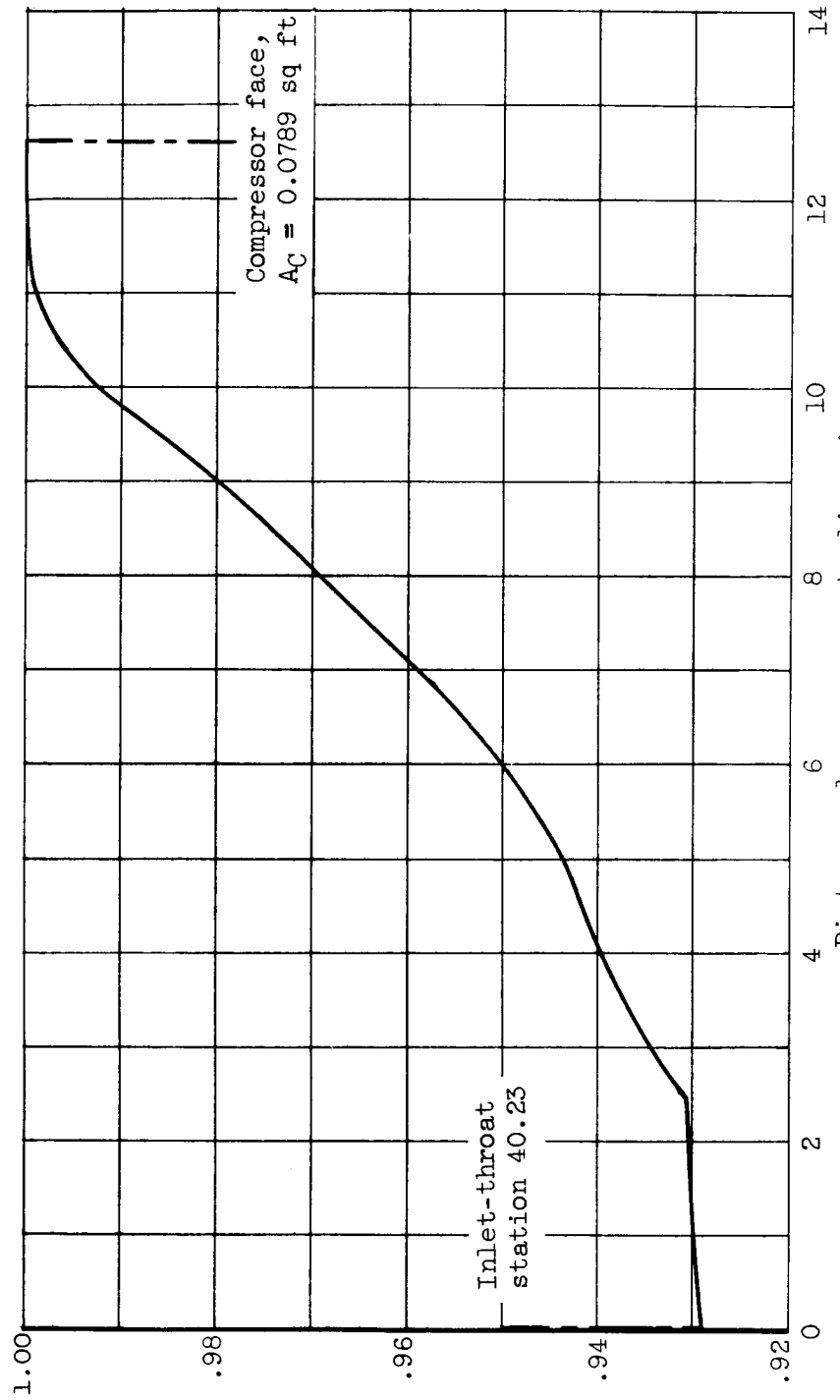

Figure 5. - Diffuser area variation.

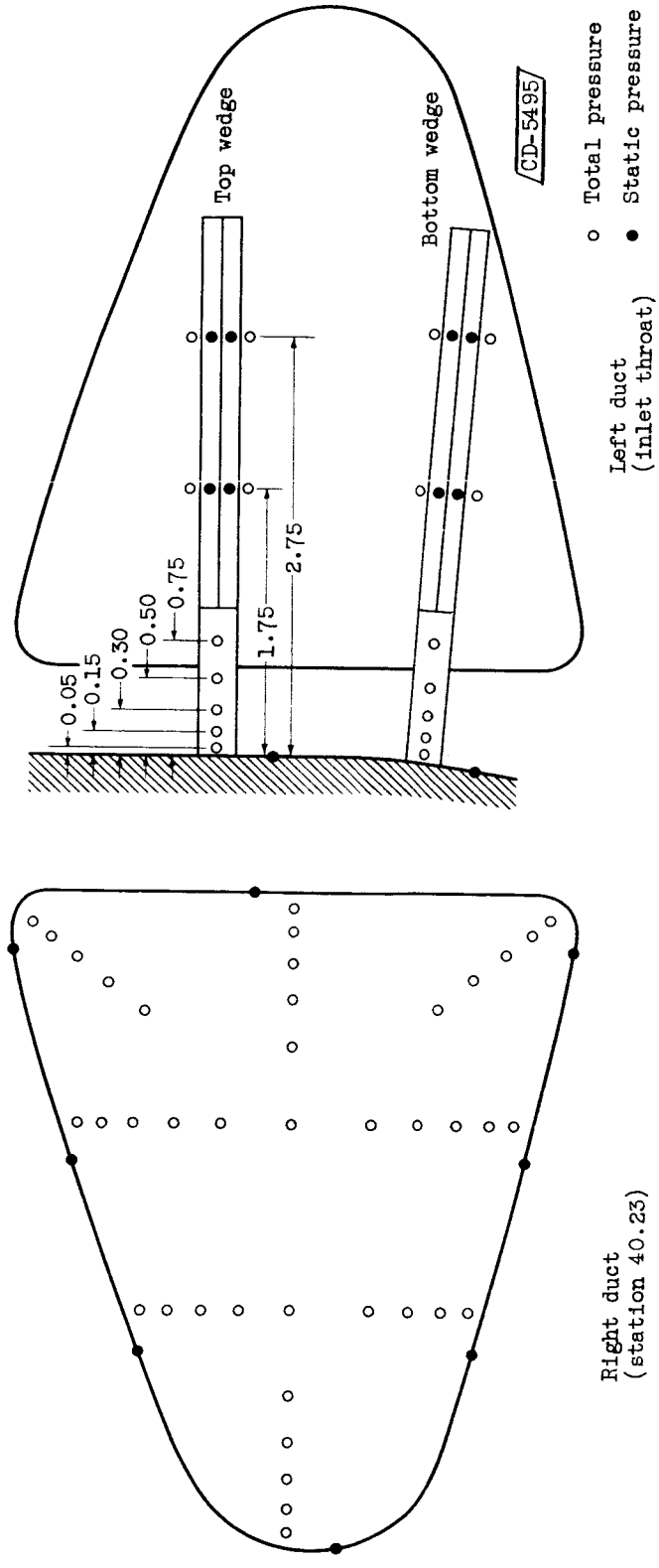

Figure 6. - Flow-survey instrumentation (dimensions in inches).

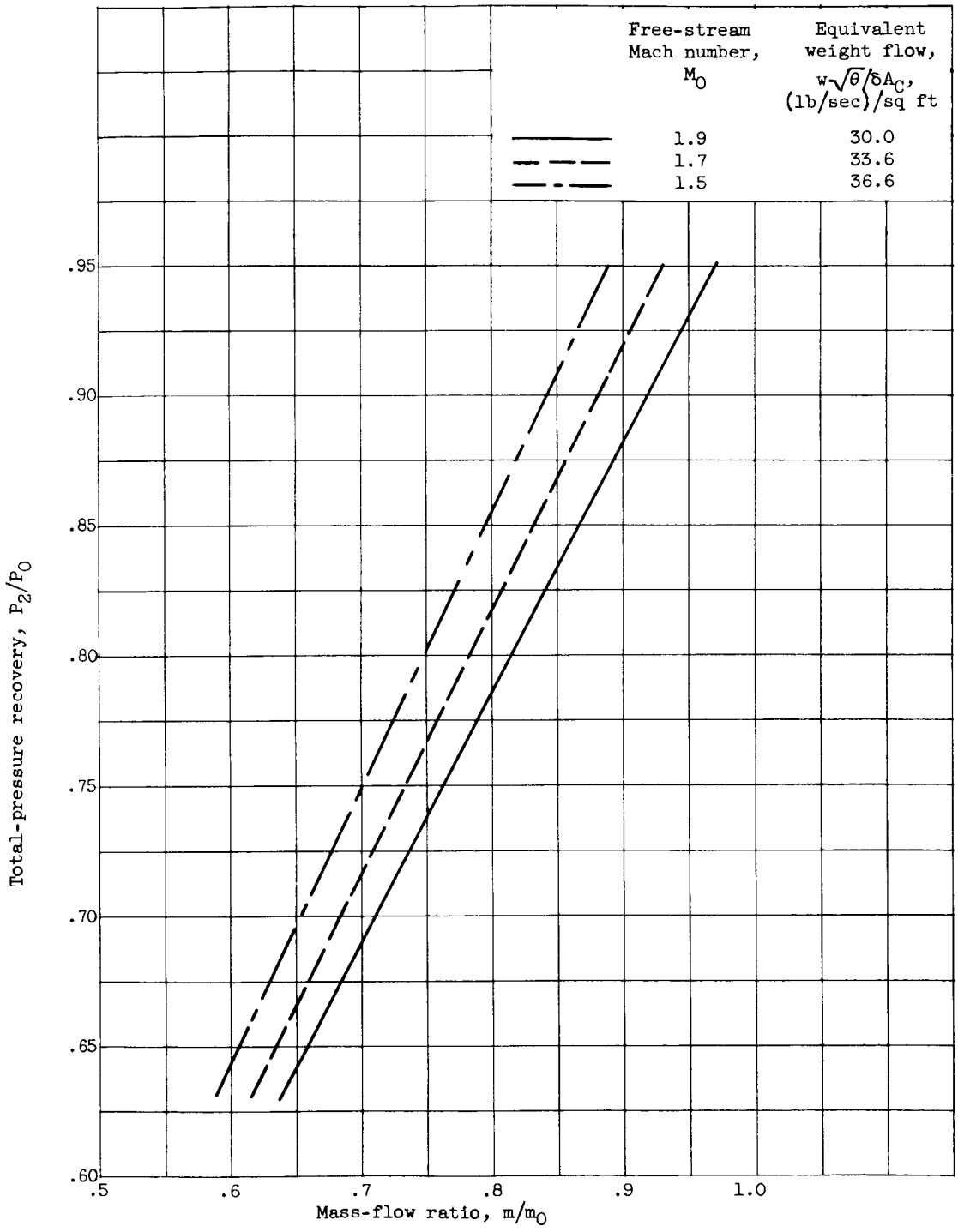

Figure 7. - Variation of mass-flow ratio with pressure recovery for 35,000-feet altitude. Matching airflow. (Mass-flow ratio based on throat area.)

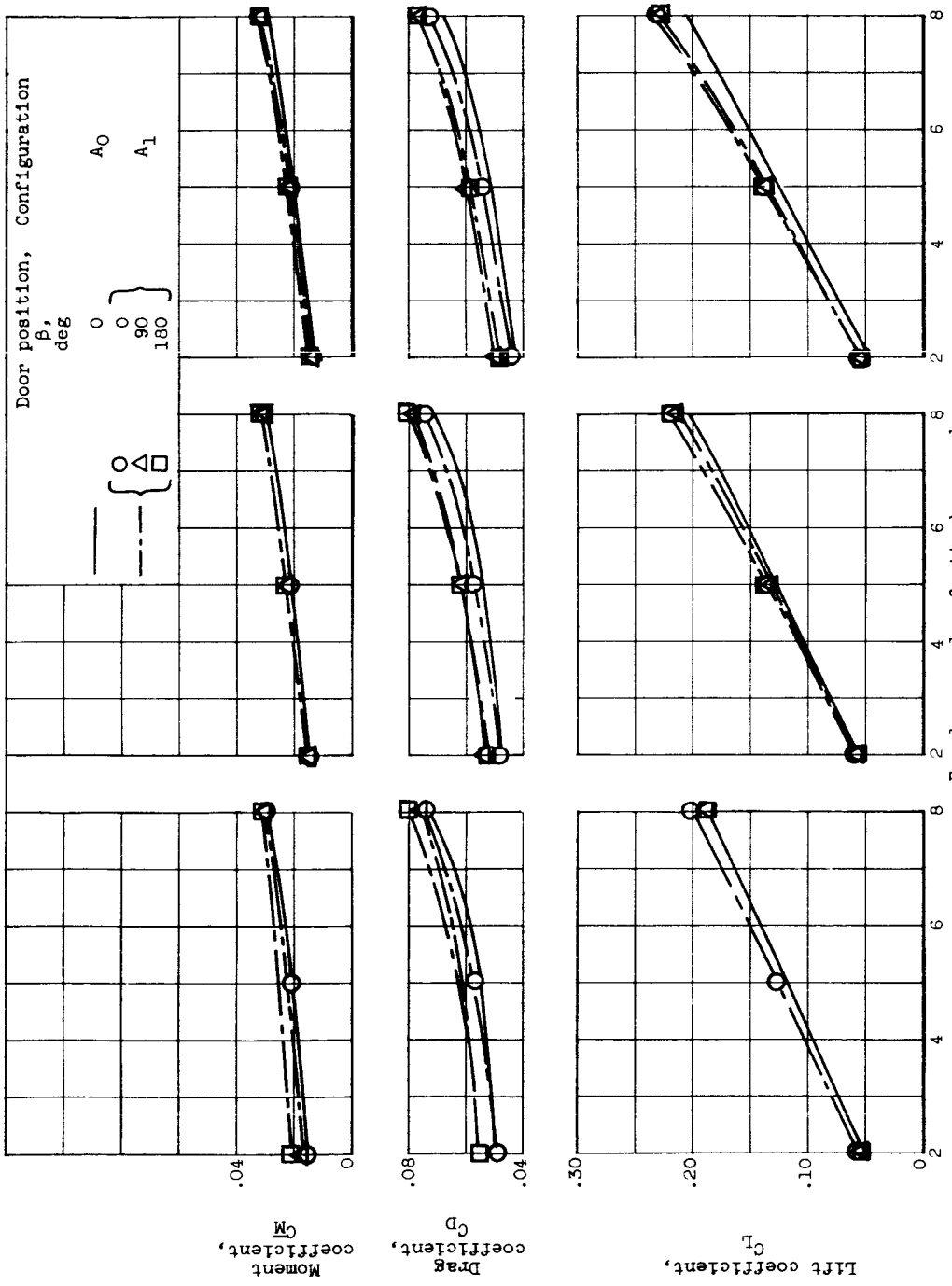

Figure 8. - Force-coefficient summary.

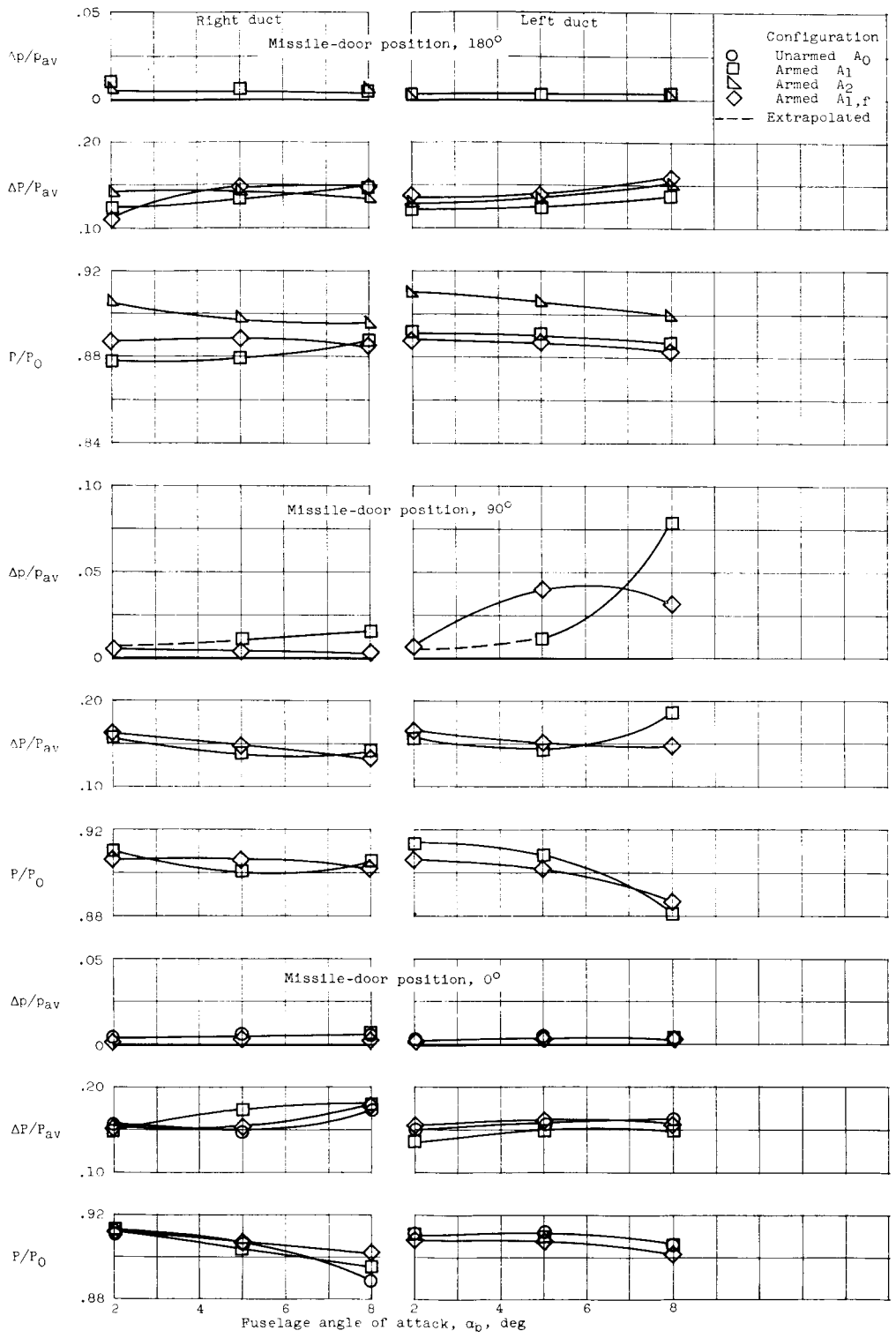

(a) Free-stream Mach number, 1.5. ($\Delta p/p_{av}$ = static-pressure fluctuation; $\Delta P/P_{av}$ = total-pressure distortion; P/P_0 = total-pressure recovery.)

Figure 9. - Performance summary of all configurations.

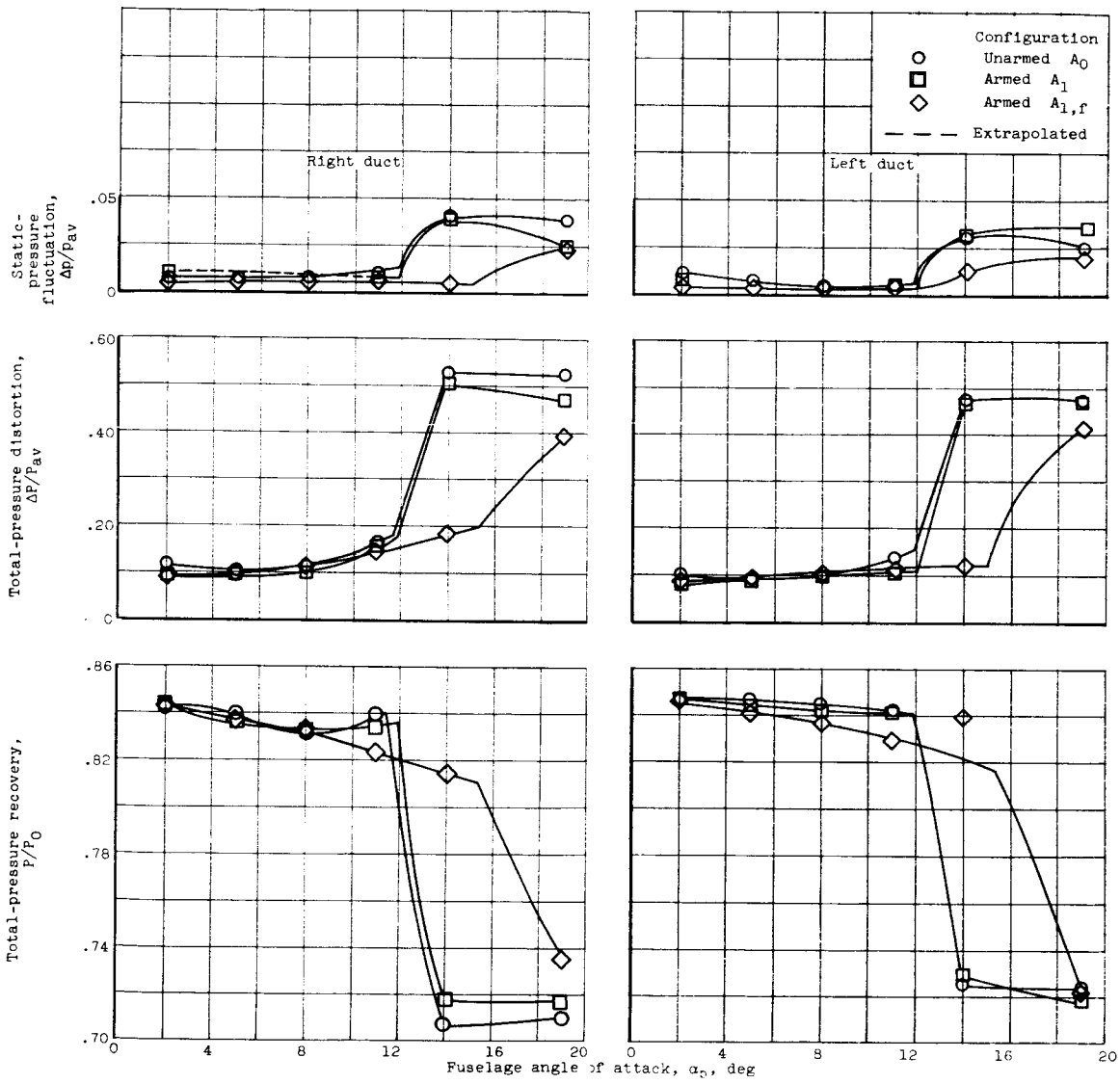

(b) Free-stream Mach number, 1.7; missile-door position, 0°.

Figure 9. - Continued. Performance summary of all configurations.

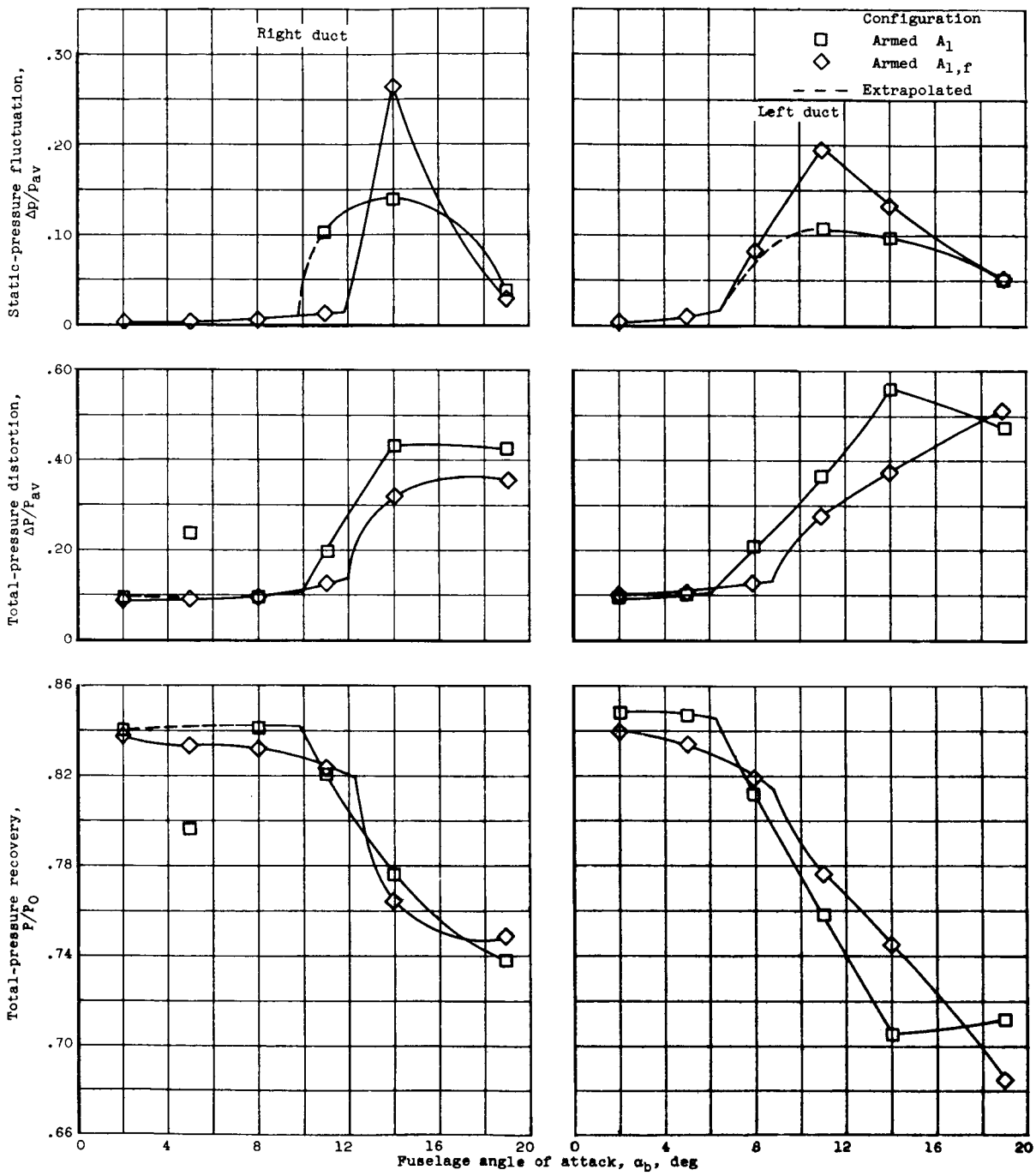

(c) Free-stream Mach number, 1.7; missile-door position, 90°.

Figure 9. - Continued. Performance summary of all configurations.

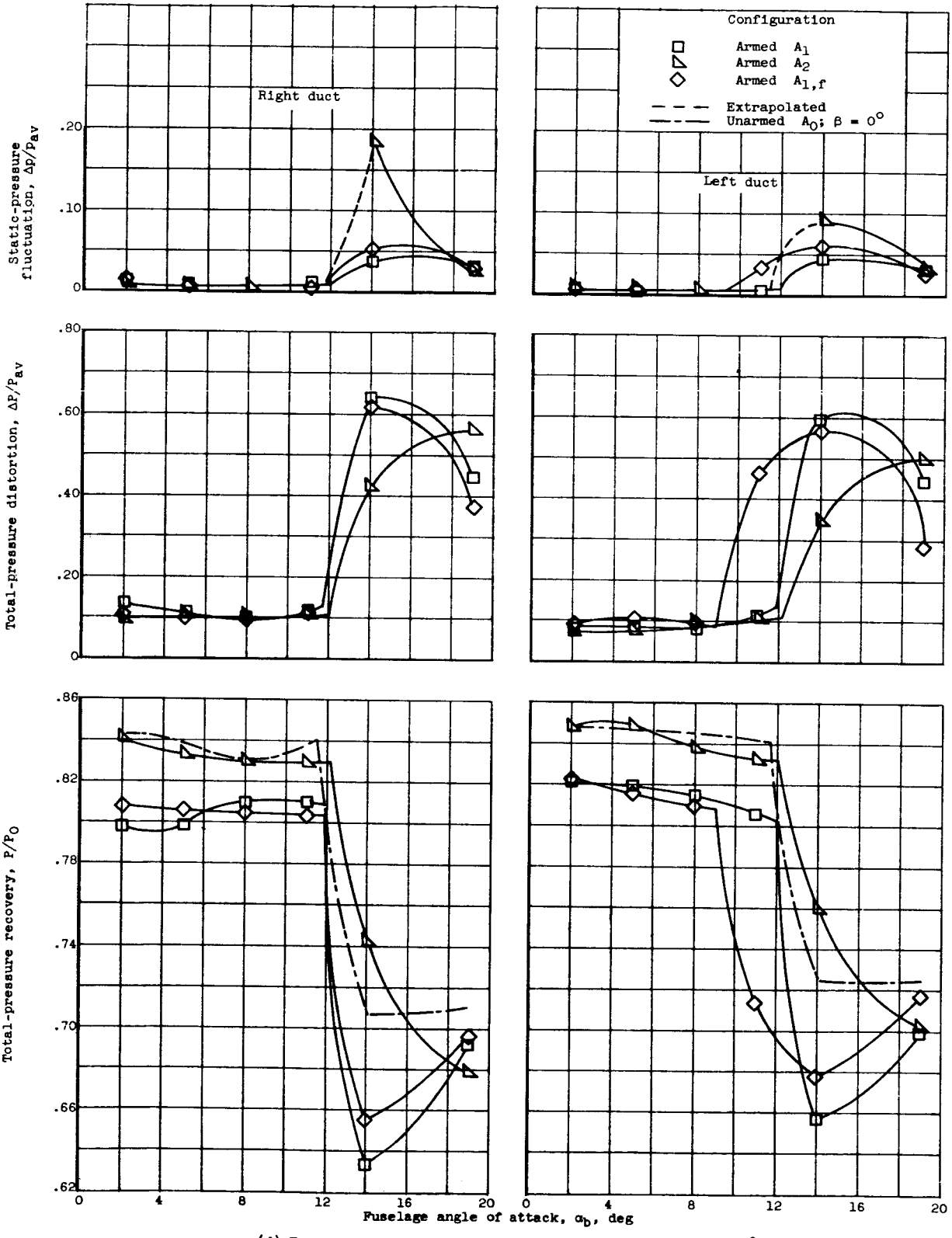

(d) Free-stream Mach number, 1.7; missile-door position, 180°.

Figure 9. - Continued. Performance summary of all configurations.

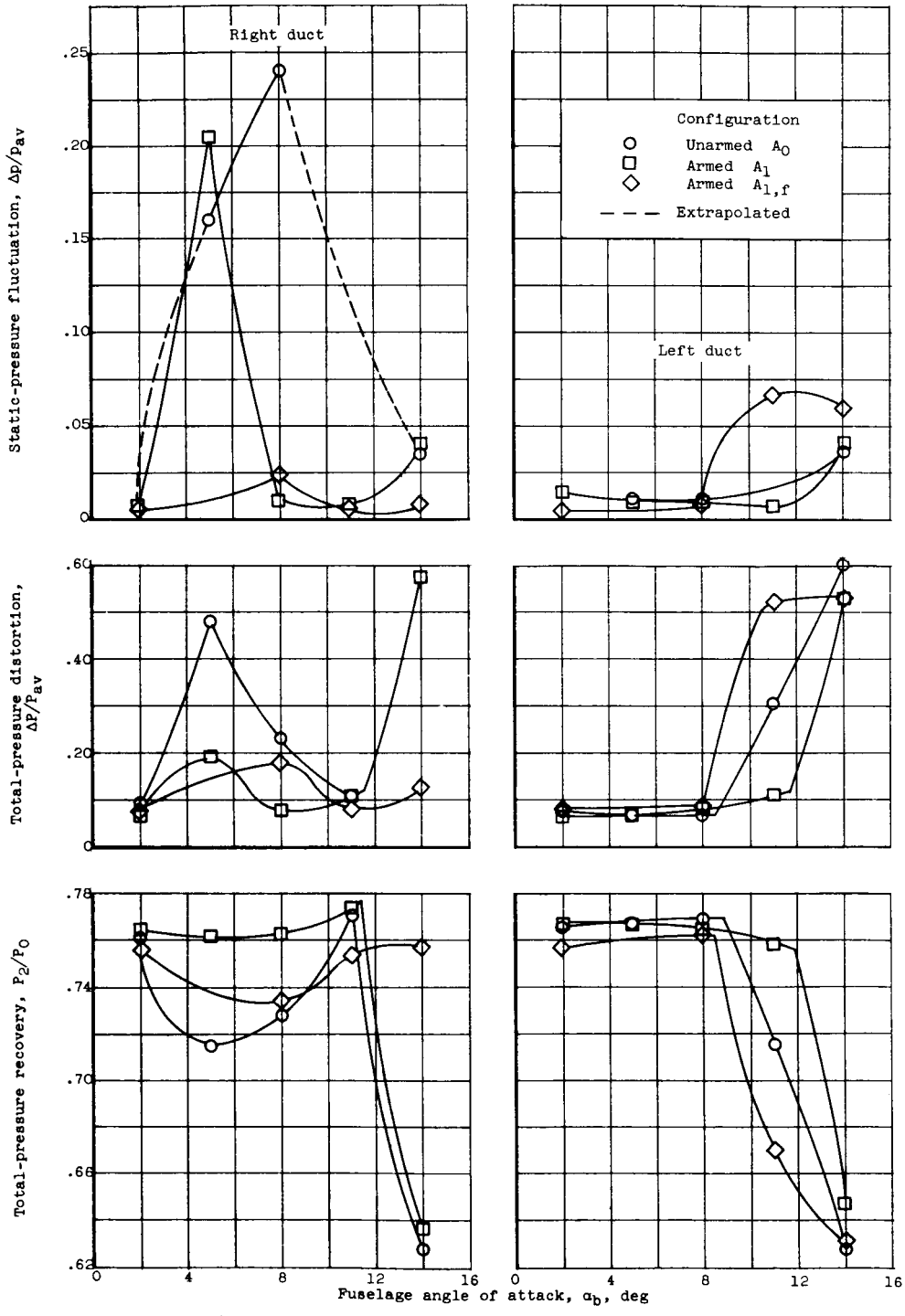

(e) Free-stream Mach number, 1.9; missile-door position, 0°.

Figure 9. - Continued. Performance summary of all configurations.

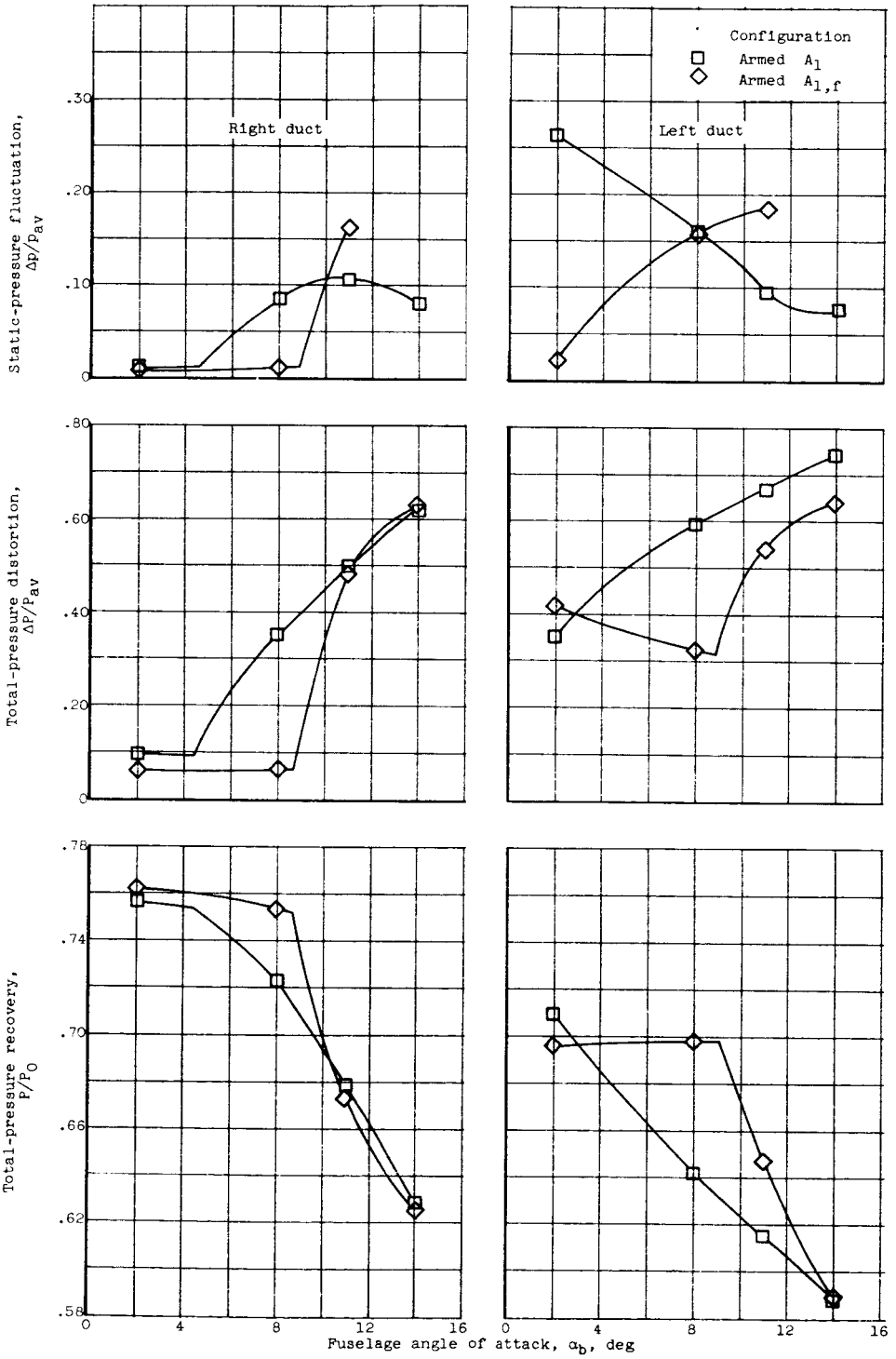

(f) Free-stream Mach number, 1.9; missile-door position, 90°.

Figure 9. - Continued. Performance summary of all configurations.

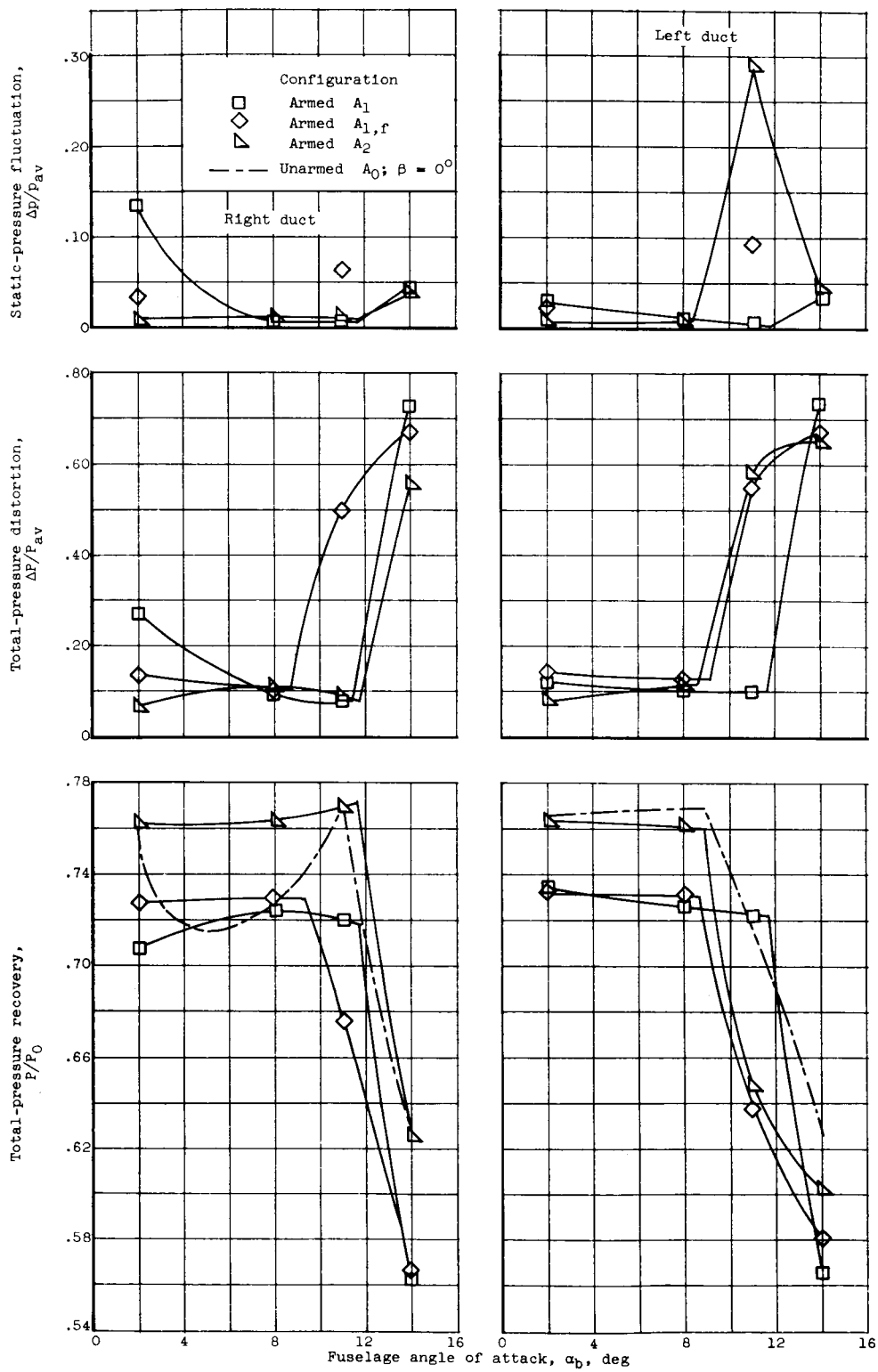

(g) Free-stream Mach number, 1.9; missile-door position, 180°.

Figure 9. - Concluded. Performance summary of all configurations.

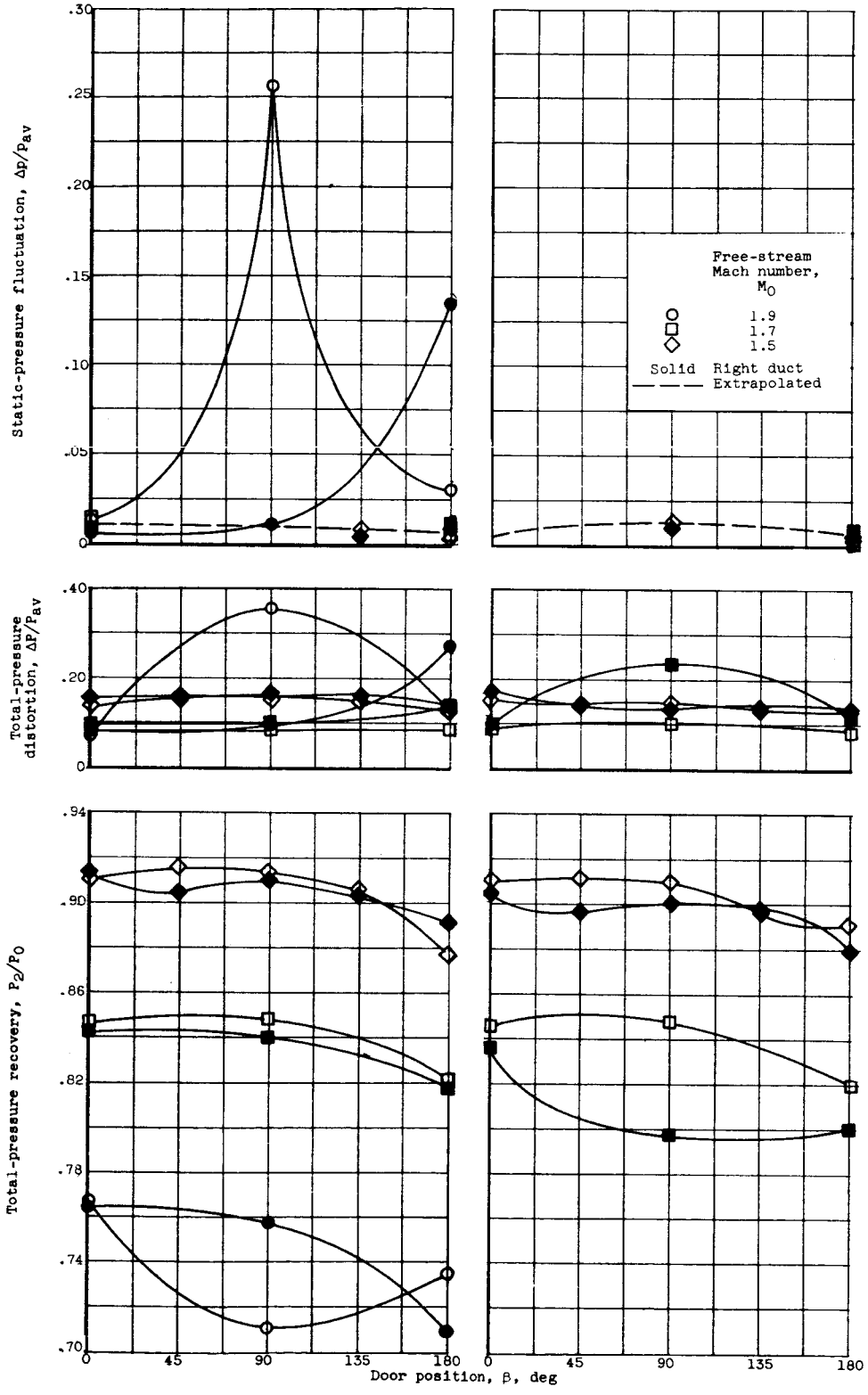

(a) Fuselage angle of attack, 2°. (b) Fuselage angle of attack, 5°.

Figure 10. - Performance summary of armed configuration A_1.

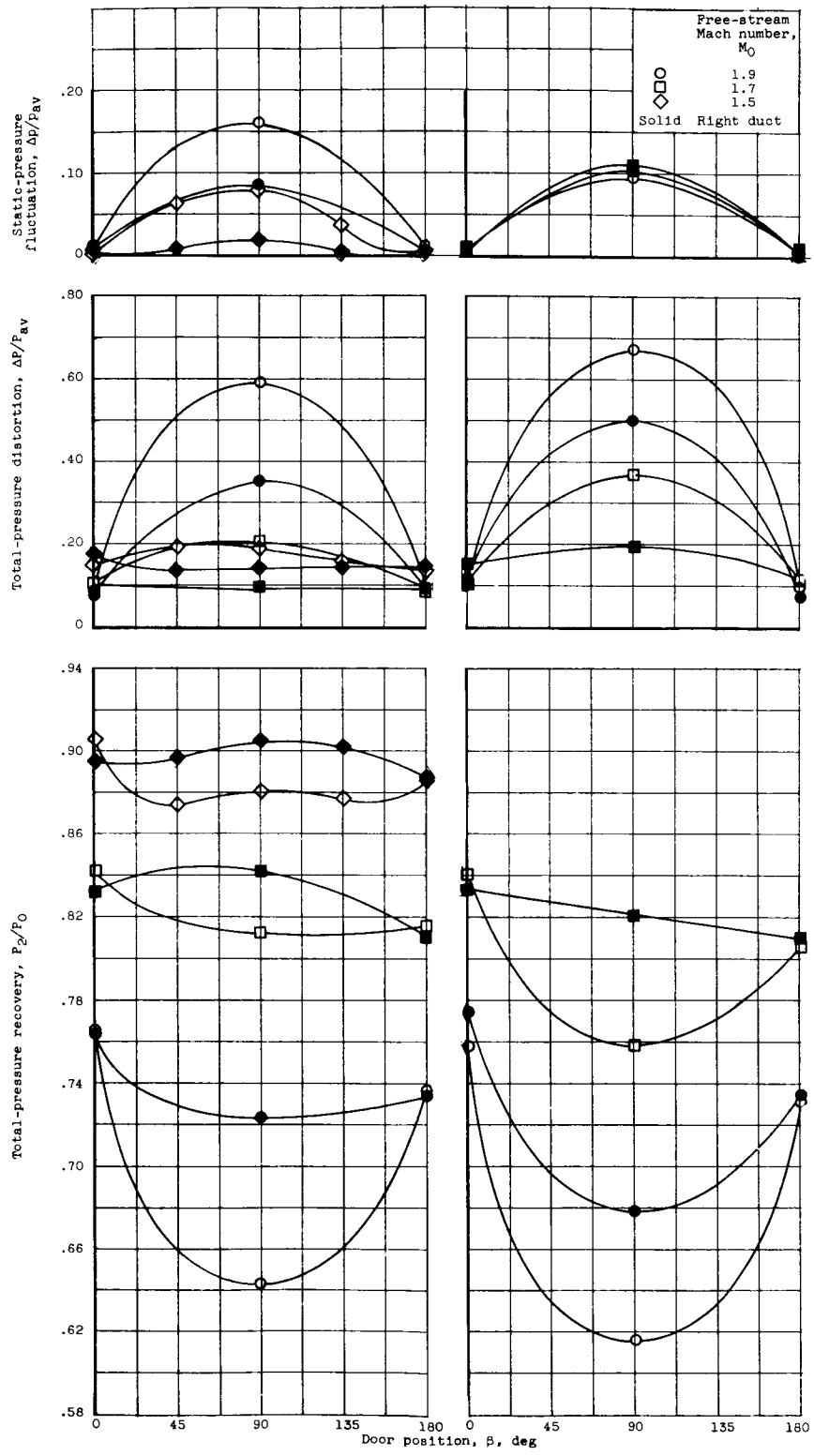

(c) Fuselage angle of attack, 8°. (d) Fuselage angle of attack, 11°.

Figure 10. - Continued. Performance summary of armed configuration A_1.

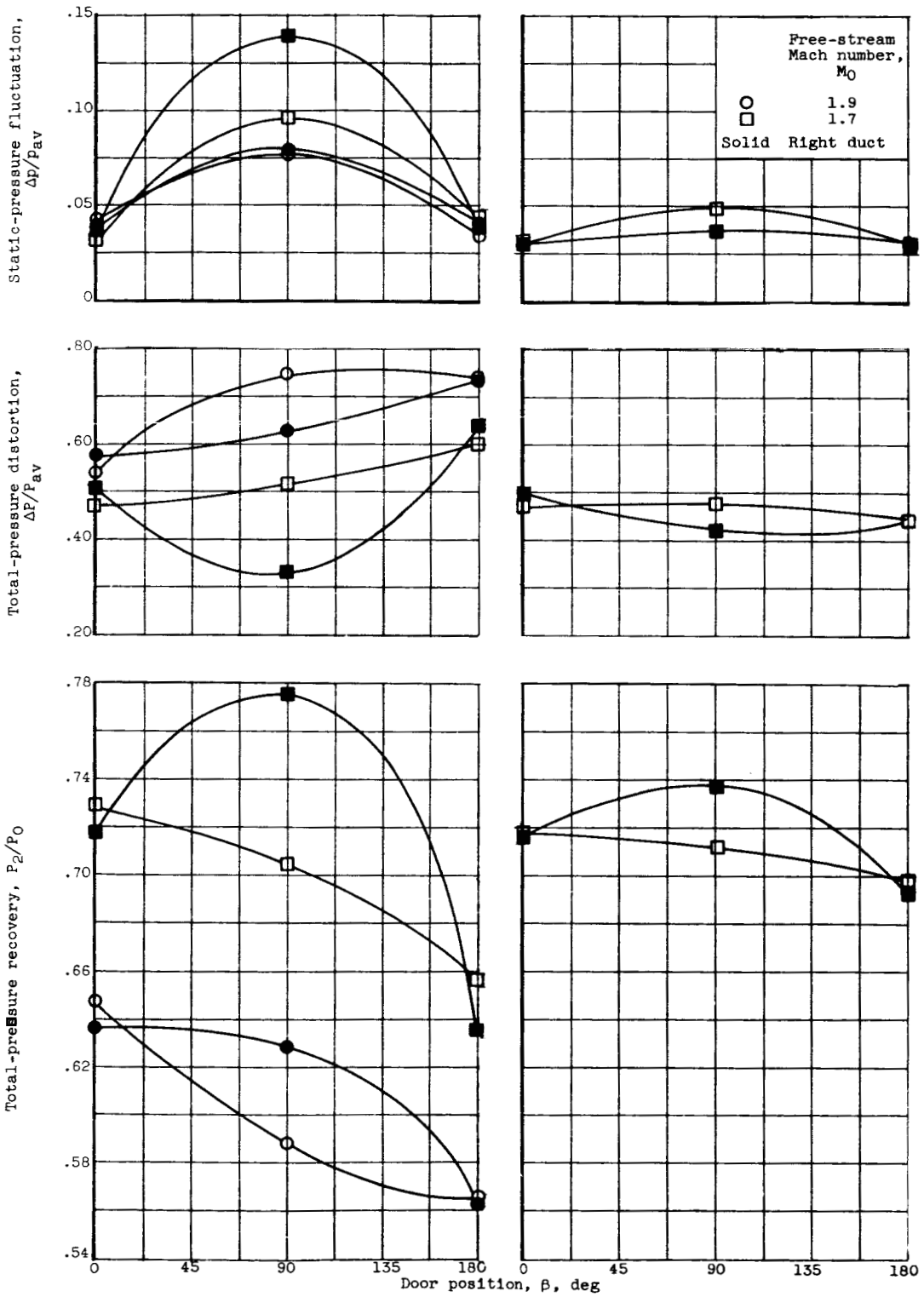

(e) Fuselage angle of attack, 14°

(f) Fuselage angle of attack, 19°.

Figure 10. - Concluded. Performance summary of armed configuration A_1.

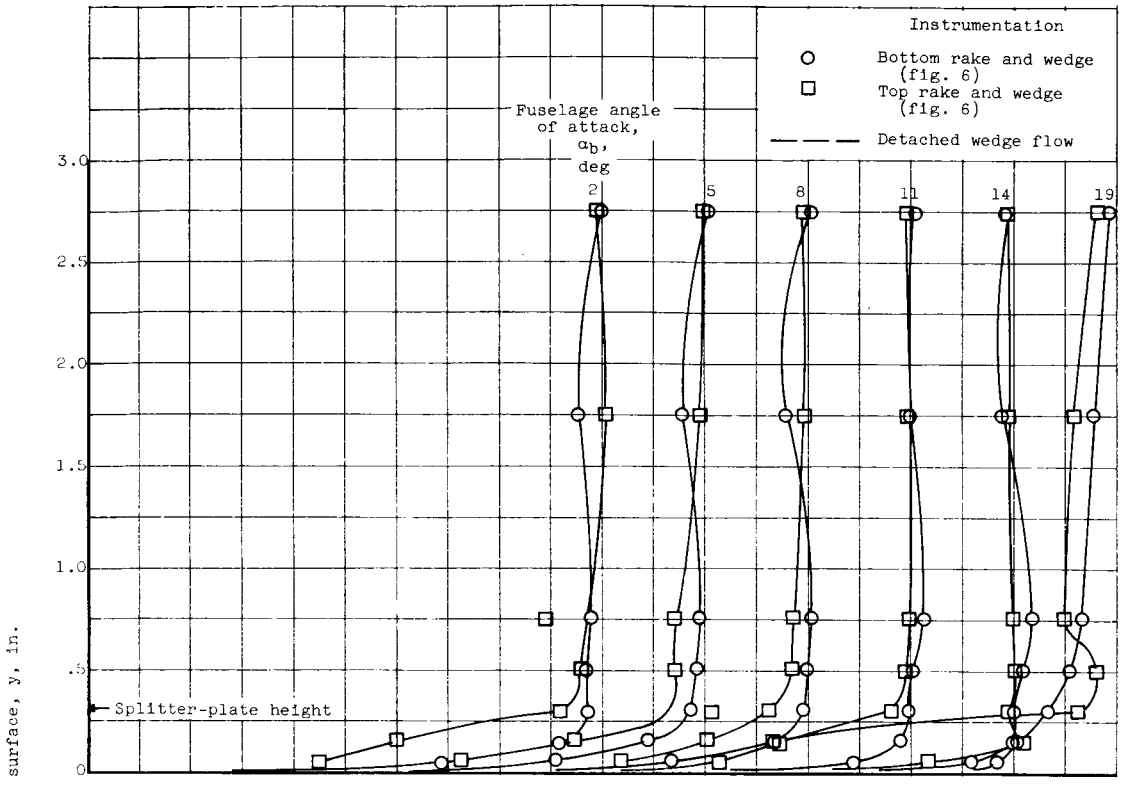

(a) Missile-door position, 0°.

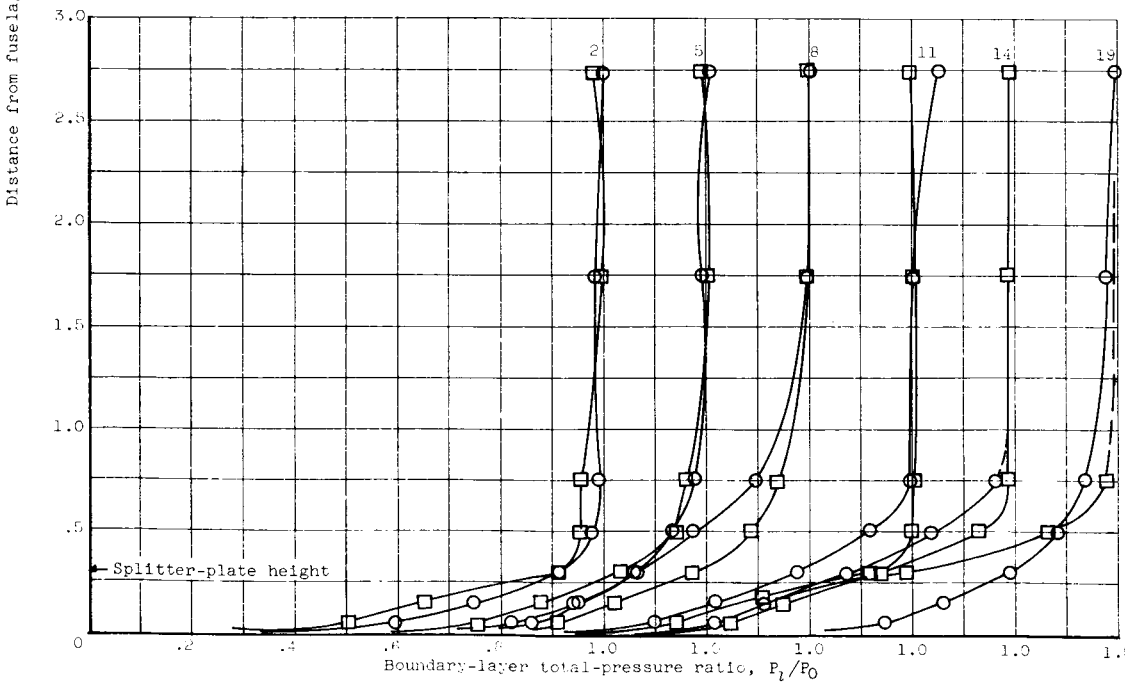

(b) Missile-door position, 90° (cavity-side inlet).

Figure 11. - Total-pressure profiles at inlet station for configuration A_1. Free-stream Mach number, 1.7.

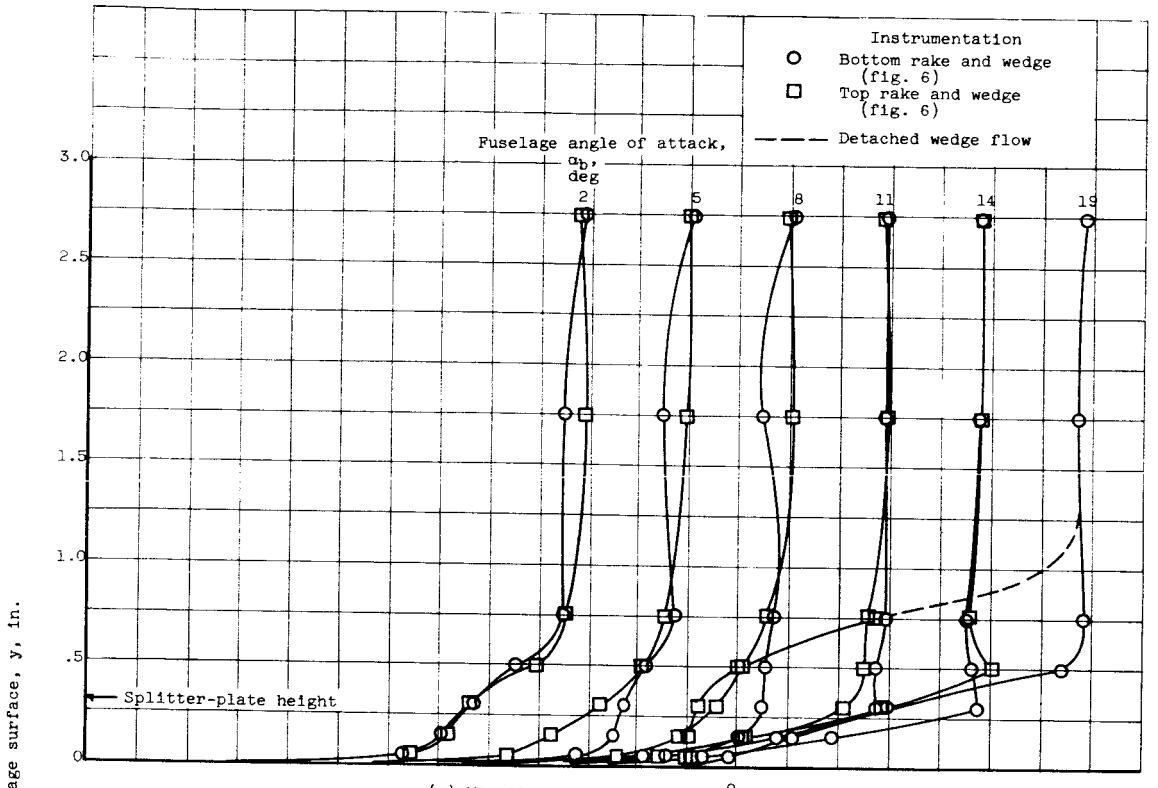

(c) Missile-door position, 180°.

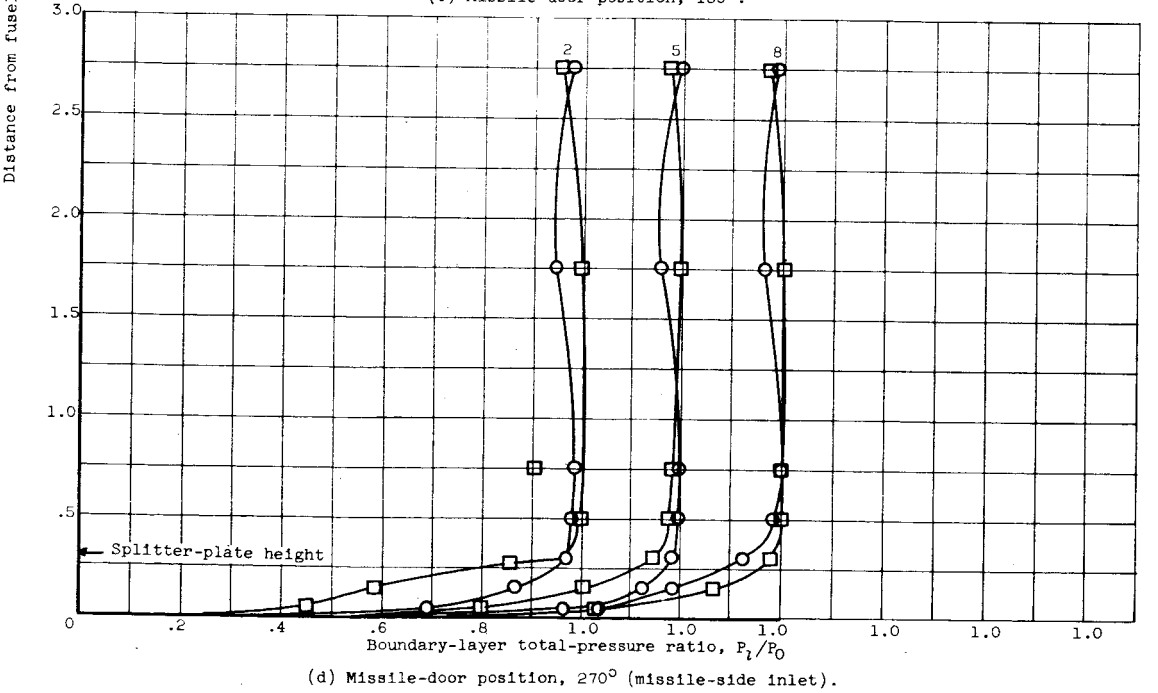

(d) Missile-door position, 270° (missile-side inlet).

Figure 11. - Concluded. Total-pressure profiles at inlet station for configuration A_1. Free-stream Mach number, 1.7.

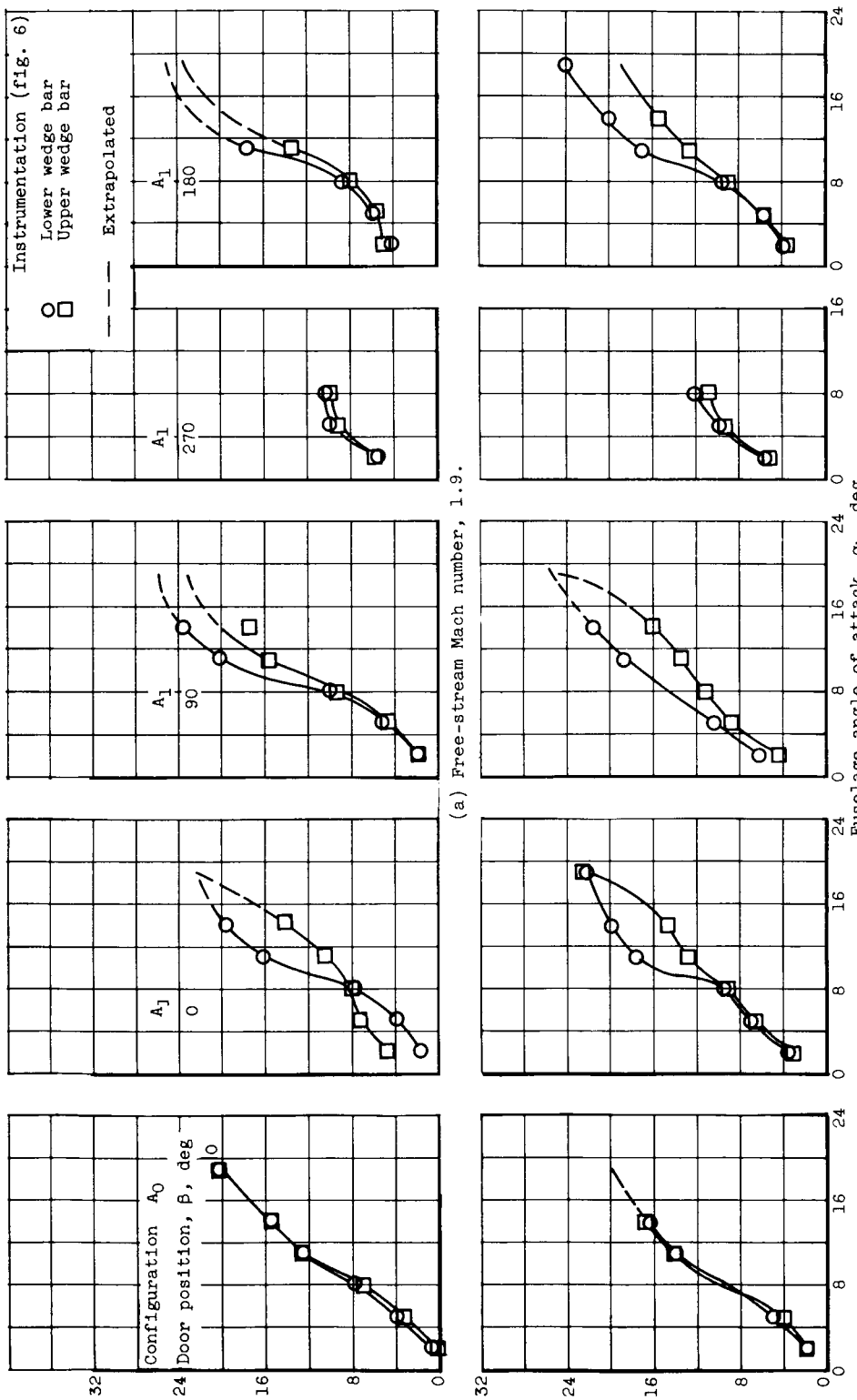

(a) Free-stream Mach number, 1.9.

(b) Free-stream Mach number, 1.7.

Figure 12. - Local flow deflections at inlet station.

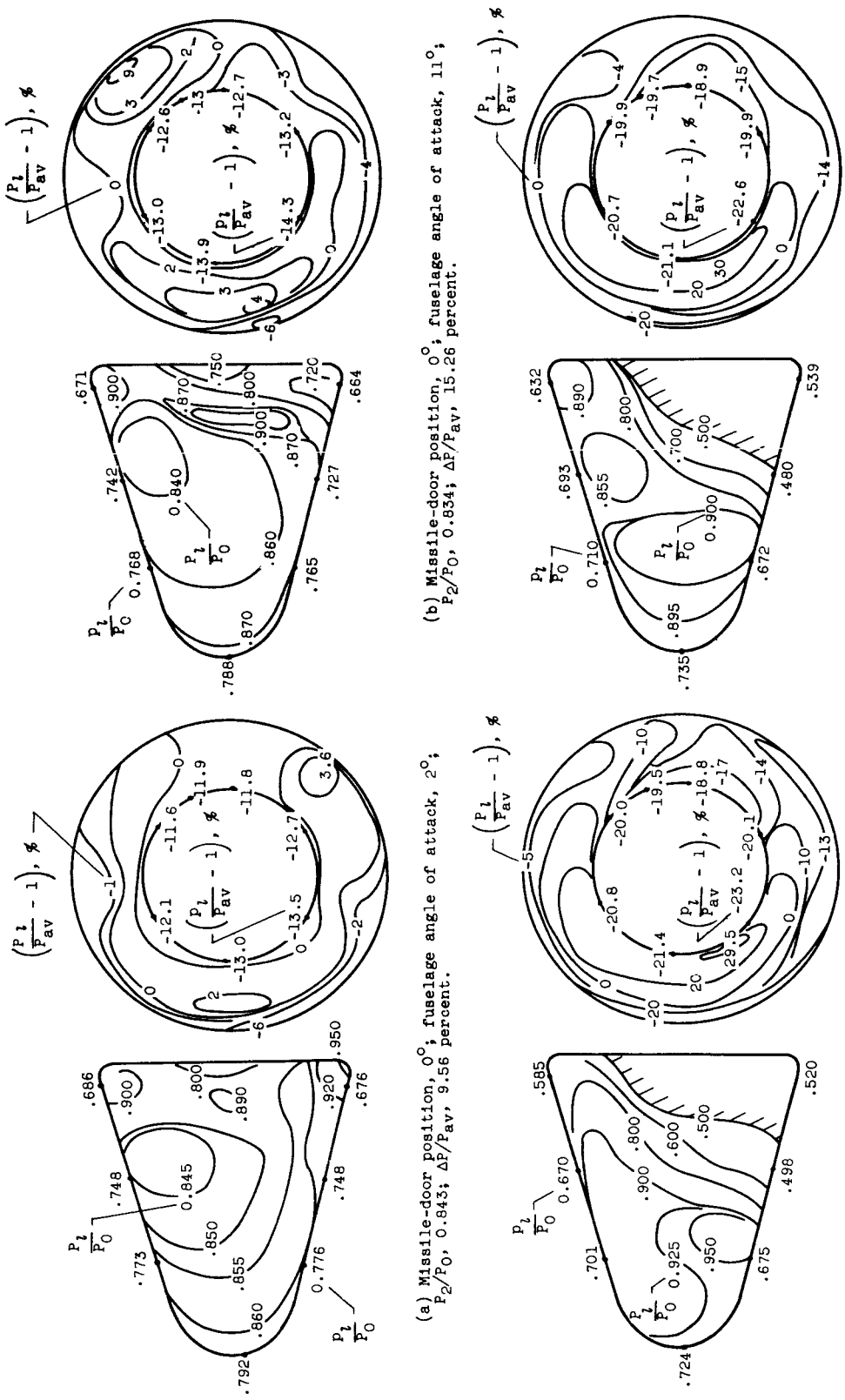

Figure 13. - Typical total-pressure contours at inlet and diffuser exit for configuration A_1. Free-stream Mach number, 1.7.

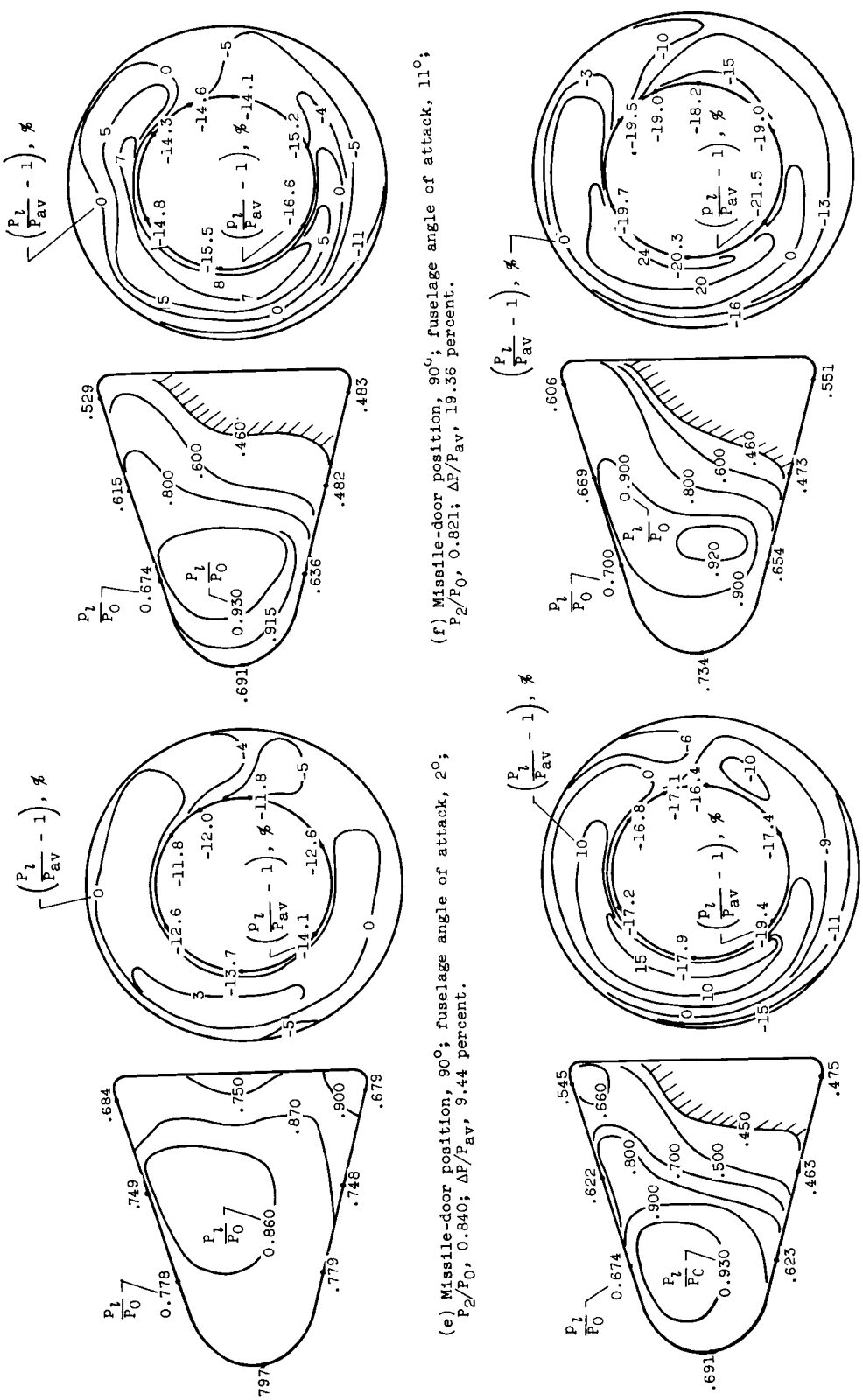

(e) Missile-door position, 90°; fuselage angle of attack, 2°; P_2/P_0, 0.840; $\Delta P/P_{av}$, 9.44 percent.

(f) Missile-door position, 90°; fuselage angle of attack, 11°; P_2/P_0, 0.821; $\Delta P/P_{av}$, 19.36 percent.

(g) Missile-door position, 90°; fuselage angle of attack, 14°; P_2/P_0, 0.776; $\Delta P/P_{av}$, 32.97 percent.

(h) Missile-door position, 90°; fuselage angle of attack, 19°; P_2/P_0, 0.738; $\Delta P/P_{av}$, 42.28 percent.

Figure 13. - Continued. Typical total-pressure contours at inlet and diffuser exit for configuration A_1. Free-stream Mach number, 1.7.

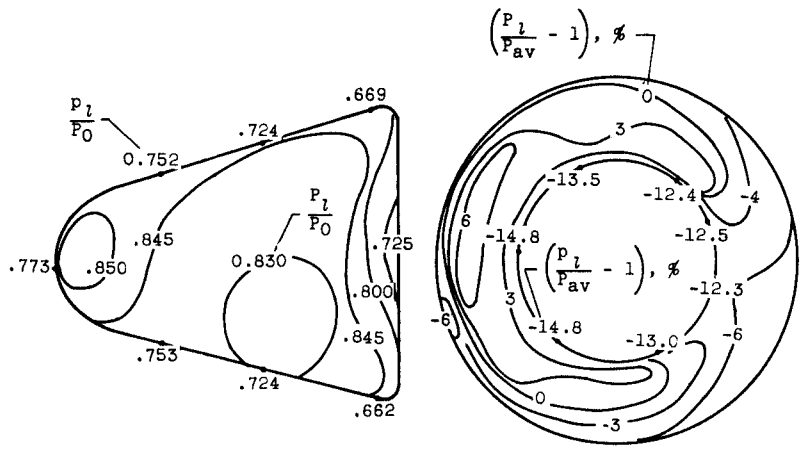

(i) Missile-door position, 180°; fuselage angle of attack, 2°; P_2/P_0, 0.824; $\Delta P/P_{av}$, 13.71 percent.

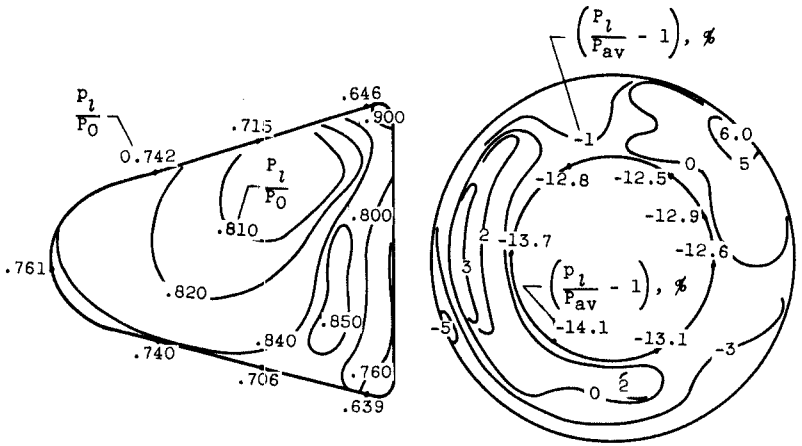

(j) Missile-door position, 180°; fuselage angle of attack, 11°; P_2/P_0, 0.810; $\Delta P/P_{av}$, 11.32 percent.

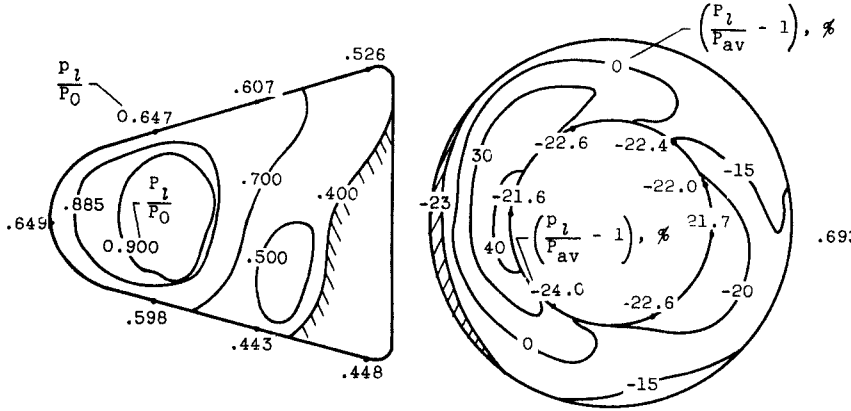

(k) Missile-door position, 180°; fuselage angle of attack, 14°; P_2/P_0, 0.635; $\Delta P/P_{av}$, 63.81 percent.

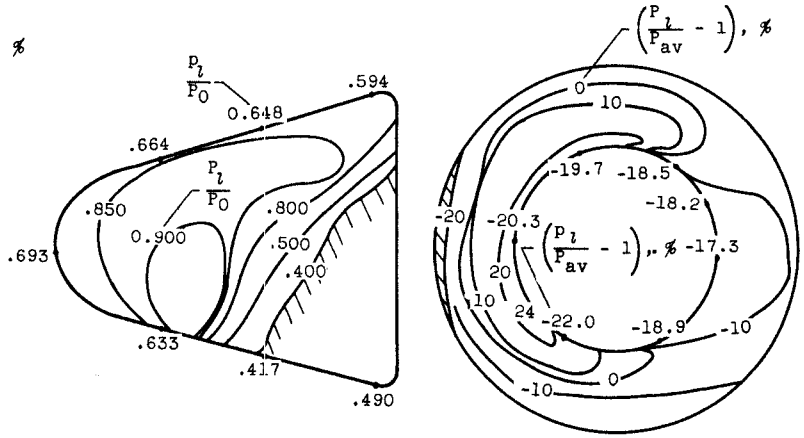

(l) Missile-door position, 180°; fuselage angle of attack, 19°; P_2/P_0, 0.692; $\Delta P/P_{av}$, 44.49 percent.

Figure 13. - Concluded. Typical total-pressure contours at inlet and diffuser exit for configuration A_1. Free-stream Mach number, 1.7.